

This discussion paper is/has been under review for the journal *Atmospheric Chemistry and Physics (ACP)*. Please refer to the corresponding final paper in *ACP* if available.

**HO_x over the tropical
rainforest: box model
results**

D. Kubistin et al.

Hydroxyl radicals in the tropical troposphere over the Suriname rainforest: comparison of measurements with the box model MECCA

D. Kubistin¹, H. Harder¹, M. Martinez¹, M. Rudolf¹, R. Sander¹, H. Bozem¹, G. Eerdeken^{1,*}, H. Fischer¹, C. Gurk¹, T. Klüpfel¹, R. Königstedt¹, U. Parchatka¹, C. L. Schiller², A. Stickler^{1,**}, D. Taraborrelli¹, J. Williams¹, and J. Lelieveld¹

¹Department of Atmospheric Chemistry, Max Planck Institute for Chemistry, Mainz, Germany

²Department of Chemistry, York University, Toronto, Canada

* now at: Department of Biology, University of Antwerp, Belgium

** now at: Institute for Atmospheric and Climate Science, ETH Zürich, Switzerland

Received: 24 June 2008 – Accepted: 15 July 2008 – Published: 12 August 2008

Correspondence to: D. Kubistin (kubistin@mpch-mainz.mpg.de)

Published by Copernicus Publications on behalf of the European Geosciences Union.

Title Page

Abstract

Introduction

Conclusions

References

Tables

Figures

◀

▶

◀

▶

Back

Close

Full Screen / Esc

Printer-friendly Version

Interactive Discussion



Abstract

As a major source region of the hydroxyl radical OH, the Tropics largely control the oxidation capacity of the atmosphere on a global scale. However, emissions of hydrocarbons from the tropical rainforest that react rapidly with OH can potentially deplete the amount of OH and thereby reduce the oxidation capacity. The airborne GABRIEL field campaign in equatorial South America (Suriname) in October 2005 investigated the influence of the tropical rainforest on the HO_x budget (HO_x=OH+HO₂). The first observations of OH and HO₂ over a tropical rainforest are compared to steady state concentrations calculated with the atmospheric chemistry box model MECCA. The important precursors and sinks for HO_x chemistry, measured during the campaign, are used as constraining parameters for the simulation of OH and HO₂. Significant underestimations of HO_x are found by the model over land during the afternoon, with mean ratios of observation to model of 12.2±3.5 and 4.1±1.4 for OH and HO₂, respectively. The discrepancy between measurements and simulation results is correlated to the abundance of isoprene. While for low isoprene mixing ratios (above ocean or at altitudes >3 km), observation and simulation agree fairly well, for mixing ratios >200 pptV (<3 km over the rainforest) the model tends to underestimate the HO_x observations as a function of isoprene.

Box model simulations have been performed with the condensed chemical mechanism of MECCA and with the detailed isoprene reaction scheme of MCM, resulting in similar results for HO_x concentrations. Simulations with constrained HO₂ concentrations show that the conversion from HO₂ to OH in the model is too low. However, by neglecting the isoprene chemistry in the model, observations and simulations agree much better. An OH source similar to the strength of the OH sink via isoprene chemistry is needed in the model to resolve the discrepancy. A possible explanation is that the oxidation of isoprene by OH not only dominates the removal of OH but also produces it in a similar amount. Several additional reactions which directly produce OH have been implemented into the box model, suggesting that upper limits in producing

ACPD

8, 15239–15289, 2008

HO_x over the tropical rainforest: box model results

D. Kubistin et al.

Title Page

Abstract

Introduction

Conclusions

References

Tables

Figures

⏪

⏩

◀

▶

Back

Close

Full Screen / Esc

Printer-friendly Version

Interactive Discussion

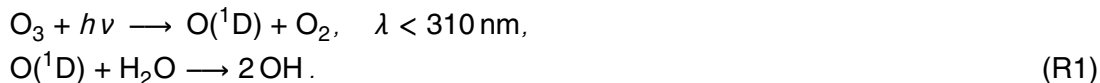


OH are still not able to reproduce the observations (improvement by factors of ≈ 2.4 and ≈ 2 for OH and HO₂, respectively). We determine that OH has to be recycled to 94% instead of the simulated 38% to match the observations, which is most likely to happen in the isoprene degradation process, otherwise additional sources are required.

1 Introduction

The hydroxyl radical (OH) and the associated hydroperoxyl radical (HO₂) play a major role in the chemistry of the troposphere, dominating its oxidation capacity during daytime. Owing to their high chemical reactivity, OH and HO₂ are responsible for the removal of most biogenic and anthropogenic trace gases, determining the lifetimes of gaseous pollutants and thereby directly impacting air quality (Heard and Pilling, 2003).

The main source of OH in the unpolluted lower troposphere is the photolysis of ozone, followed by the reaction with water vapour (Levy, 1971):



Therefore OH production rates are largest in tropical regions, where humidity and irradiation intensity are high (Lelieveld et al., 2002).

On the other hand, emissions of biogenic trace gases are controlled by solar radiation and temperature (Kesselmeier and Staudt, 1999; Fuentes et al., 2000). Tropical regions naturally have large areas of rainforest and these ecosystems represent a major source of volatile organic compounds (VOC) on a global scale (Fehsenfeld et al., 1992; Guenther et al., 1995). Global models typically predict a large influence from the tropical rainforest VOC emissions on the hydroxyl radical concentration (Logan et al., 1981; Karl et al., 2007) by the reaction:



HO_x over the tropical rainforest: box model results

D. Kubistin et al.

Title Page

Abstract

Introduction

Conclusions

References

Tables

Figures

◀

▶

◀

▶

Back

Close

Full Screen / Esc

Printer-friendly Version

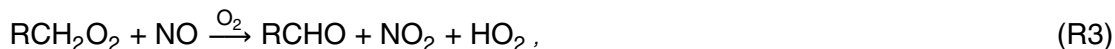
Interactive Discussion



which has been thought to suppress OH and the oxidation capacity of the atmosphere (Wang et al., 1998; Poisson et al., 2000; Lelieveld et al., 2002; Kuhlmann et al., 2004; Joeckel et al., 2006). The main biogenic volatile organic compound (BVOC) emitted from the tropical rainforest is isoprene (Guenther et al., 1995; Granier et al., 2000).

5 Many laboratory based oxidation experiments of isoprene with OH have been performed (e.g. Paulson et al., 1992; Jenkin et al., 1997) and a detailed degradation scheme can be found in Jenkin and Hayman (1995).

The peroxy radicals generated in the initial step can further react with nitric oxide (NO), forming the hydroperoxyl radical, HO₂:



which can recycle OH via reaction with nitric oxide or ozone:



The two radical species OH and HO₂ can be considered to be in photochemical equilibrium on a timescale of seconds (Eisele et al., 1994).

10 The objective of the airborne GABRIEL campaign (**G**uyanans **A**tmosphere-**B**iosphere Exchange and **R**adicals **I**ntensive **E**xperiment with the **L**earjet) was to study how the VOC emissions from the pristine rainforest in equatorial South America influence the HO_x (HO_x=OH+HO₂) budget. In this study, the impact of BVOCs on the HO_x budget is investigated by comparing the measurements with an observationally constrained box model in steady state. The differences between model and observations for HO_x are analysed and possible modifications of the chemical reaction scheme are discussed.

2 Measurements

The GABRIEL campaign took place over Suriname, French Guiane and Guyana (3° to 6° N, 51° to 59° W). This region is sparsely populated and mainly characterised by pris-

HO_x over the tropical rainforest: box model results

D. Kubistin et al.

Title Page

Abstract

Introduction

Conclusions

References

Tables

Figures

◀

▶

◀

▶

Back

Close

Full Screen / Esc

Printer-friendly Version

Interactive Discussion



HO_x over the tropical rainforest: box model results

D. Kubistin et al.

Title Page

Abstract

Introduction

Conclusions

References

Tables

Figures

◀

▶

◀

▶

Back

Close

Full Screen / Esc

Printer-friendly Version

Interactive Discussion

tine rainforest. Flights were performed from Zanderij Airport, Suriname (5° N, 55° W) in October 2005, during the long dry season (August–November). The prevailing wind direction during the campaign was from the tropical Atlantic Ocean towards the rainforest (southeasterly trade winds). The wind therefore transported clean background maritime air over the forested regions of the Guyanas. Flights were performed to sample air at various altitudes (300 m–9 km) and at different distances from the coast (Fig. 1), hence determining the extent of biogenic influence. The flights were conducted at different times of the day (Table 1), since the primary production of OH in the troposphere is light dependent (R1), as are the emissions of trace gases from the rainforest (Fuentes et al., 2000).

All species relevant for fast photochemistry were measured in-situ on board a Learjet 35A D-CGFD (GFD¹). OH was directly detected by the laser induced fluorescence (LIF) technique, whereas HO₂ was quantified indirectly by conversion to OH via addition of NO (Martinez et al., 2008). These are the first reported observations of HO_x over the tropical rainforest (Lelieveld et al., 2008). The time resolution of the measurements varied from one to 30 s. An overview of the measured species is given in Table 2.

The measured HO_x data is shown in Figs. 2 and 3. The data (30 s average) was binned in 3-h time intervals to distinguish between morning, noon and afternoon conditions. Local time is UTC (Universal Time Coordinates) minus 3 h. The 1σ uncertainty of the OH and HO₂ measurements was estimated to be 20% and 30% by the systematic error and 7% and 1% by the statistical error (as mean value), respectively. A more detailed description can be found in Martinez et al. (2008).

The influence of the rainforest emissions in the boundary layer (<1000 m) is illustrated by the decrease in the OH concentration in the air mass travelling from the ocean to the land. As the VOC accumulate in the atmosphere over the rainforest, they reduce OH and contribute to HO₂ production.

To quantify our understanding of the tropospheric chemical processes in more detail, comparisons with box model calculations have been performed. It will be shown that,

¹Gesellschaft für Flugzieldarstellung, Hohn, Germany.



although OH concentrations decreased over the rainforest, this decrease was much less than expected and possible explanations will be discussed.

3 Box model

The comparison of observed data with chemical box model calculations helps to improve our understanding of the atmospheric oxidation mechanisms. For our analysis, the photochemical box model MECCA (**M**odule **E**fficiently **C**alculating the **C**hemistry of the **A**tmosphere) was used to simulate OH and HO₂. The chemical reaction scheme is based on MECCA v0.1p (Sander et al., 2005) containing the “Mainz Isoprene Mechanism” (MIM) (Poeschl et al., 2000) with 44 reactions and 16 organic species describing the chemistry of isoprene. The maximum number of species in the gas phase is 116 with a total number of 295 reactions. For the simulations, the halogen, sulfur and aqueous phase reactions were neglected and the multiphase chemistry, represented as heterogeneous loss, was only considered in order to represent the deposition of peroxides. The detailed reaction scheme can be found in the accompanying supplement (<http://www.atmos-chem-phys-discuss.net/8/15239/2008/acpd-8-15239-2008-supplement.pdf>).

MIM is a reduced reaction scheme in which different species belonging to a class (e.g. carbonyls, peroxy radicals, peroxides and organic nitrates) are lumped into groups of VOC. To verify the influence of the most abundant nonmethane hydrocarbons (NMHC) over the tropical rainforest, the comprehensive isoprene degradation scheme of the Master Chemical Mechanism MCM 3.1 (Jenkin et al., 1997; Saunders et al., 1997, 2003) was also used in our studies.

The photolysis frequencies (J) were determined using the radiative transfer model TUV v4.1 (**T**ropospheric **U**ltraviolet-**V**isible Model) (Madronich and Flocke, 1998) with a total ozone column of 265 DU (GOME satellite data). The cross sections and quantum yields for the different species were taken from the recommended data of Atkinson et al. (2004, 2005) and Sander et al. (2006). The calculated photolysis frequencies were

HO_x over the tropical rainforest: box model results

D. Kubistin et al.

Title Page

Abstract

Introduction

Conclusions

References

Tables

Figures

◀

▶

◀

▶

Back

Close

Full Screen / Esc

Printer-friendly Version

Interactive Discussion



corrected for cloud and aerosol effects by scaling to the measured $J(\text{NO}_2)$.

Considering the short lifetimes of OH and HO_2 radicals, all model runs were performed to reach steady state. To constrain the model runs, the measured species during the GABRIEL campaign were fixed to their observed values with a time resolution of 2 min. Trace gases which were not measured were either calculated by the model or taken as fixed parameters as given in Table 3. Although the instruments generally operated steadily and reliably during the GABRIEL campaign, some short interruptions, calibrations or malfunctions did occur. As nitric oxide (NO) is a crucial parameter for the HO_x cycling, datasets without NO data were omitted from this study (flights G01, G05 and G10). For water vapour and carbon monoxide, missing data points were interpolated within 2 min intervals for equal altitude levels. For two flights (G02, G07) water data were not available. As H_2O concentration correlates with altitude and the day-to-day variability was small, the mean vertical profile of water from the 8 other flights was used as a proxy to fill in the missing data. The uncertainty was derived from the standard deviation of the mean profile (Fig. 4). For hydrogen peroxide (H_2O_2), missing data were simulated by using an altitude dependent heterogeneous removal rate function, which was fitted to loss rates determined by the model to match the measured data where available (Fig. 5). This loss rate is in reasonably good agreement with calculated deposition rates by Stickler et al. (2007), who determined deposition rates in the boundary layer of $1.35 \times 10^{-5} \dots 4 \text{ s}^{-1}$ for the tropical rainforest and about $3.25 \times 10^{-5} \text{ s}^{-1}$ for the tropical Atlantic. Total organic peroxides (ΣROOH) were modelled by using the same removal rates as for H_2O_2 . Comparison of the simulated and measured data shows a slight underestimation of hydrogen peroxide and overestimation of total organic peroxides (Fig. 6). For altitudes higher than 5.5 km, measurements of total peroxides and H_2O_2 could not be carried out (Stickler et al., 2007). These missing data were simulated with a removal rate of zero (Jackson and Hewitt, 1999). Altogether, the whole dataset used for the simulation of OH and HO_2 consists of 140 data points, corresponding to 280 min of data. The dataset from the direct measurements predominately comprises regions over land in the afternoon

HO_x over the tropical rainforest: box model results

D. Kubistin et al.

Title Page

Abstract

Introduction

Conclusions

References

Tables

Figures

◀

▶

◀

▶

Back

Close

Full Screen / Esc

Printer-friendly Version

Interactive Discussion



at low altitudes (Fig. 7). Datasets for the morning and for high altitudes could only be established based on the assumptions described above and accordingly have a larger uncertainty. Model simulations which used these more uncertain datapoints are marked separately (triangles). Nevertheless, the overall uncertainty for the modelling of HO_x as caused by these assumptions is less than 50%. Uncertainties originating from the inaccuracies of the kinetic rate coefficients are not considered here.

4 Results and discussion

To examine the radical chemistry over the tropical rainforest, diverse tropospheric conditions (e.g. time of day, altitude, background air) were covered by the flighttracks performed during GABRIEL. Air influenced by rainforest emissions as well as unaffected air over the ocean was sampled. Figure 8 shows the observed to modelled ratio for OH and HO_2 as a function of location. Over the ocean and at higher altitudes the agreement is fairly good for OH and HO_2 with a possible slight model underestimation of OH and an overestimation of HO_2 . However over the rainforest at low altitudes, where the emission of hydrocarbons influences the chemistry, the divergence between model and observation increases strongly. These discrepancies are greater for the hydroxyl radical (up to factors of 15) than for HO_2 (up to factors of 5). The substantial underestimation is an indication of the inadequacy of the hydrocarbon chemistry scheme adopted in the model.

The uncertainty estimation for observations and simulations are included in the analyses to define the significance of the discrepancies. Figure 9 shows the 1σ range of the observed and modelled data, derived from the measurement uncertainties of the species that constrain the model. Upper and lower estimates are obtained by varying all concentrations within the uncertainties to achieve maximum and minimum production of OH and HO_2 , and conversion of HO_2 to OH. Although OH and HO_2 concentrations were often reproduced by the model within a factor 2, there was significant disagreement for several data points for which the simulated values were lower than

HO_x over the tropical rainforest: box model results

D. Kubistin et al.

Title Page

Abstract

Introduction

Conclusions

References

Tables

Figures

◀

▶

◀

▶

Back

Close

Full Screen / Esc

Printer-friendly Version

Interactive Discussion



the observations.

Further sensitivity studies of the model have been performed including the constraining parameters to identify the observed trace gases with the strongest influence on the HO_x concentrations by varying the concentrations of the single observed species separately by factors ranging from 0 and 3. Their influence on the HO_x concentration is shown for afternoon data over the rainforest in Table 4. The strongest sensitivities with respect to OH result from ozone photodissociation and subsequent reaction with water vapour (163% and 145%, respectively), responsible for the primary production, and from isoprene (150%). The simulations of HO₂ are less sensitive to the applied variations, with the largest influence from formaldehyde (136%). Thus, the variation of any single constrained parameter by a factor of 2 is not sufficient to eliminate the discrepancy between the simulated and observed OH and HO₂ concentrations.

4.1 Correlation with isoprene

Comparison between observations and model simulations for OH and HO₂ with respect to the diurnal cycle, shows that model underestimations are relatively large in the afternoon, especially in the boundary layer (Fig. 10). Emissions of hydrocarbons from the rainforest are driven by light and temperature. The most abundant VOC species over the rainforest is isoprene (Guenther et al., 1995; Granier et al., 2000), the concentration of which increases strongly towards the afternoon (Fig. 11) (Eerdekens et al., 2008; Warneke et al., 2001). The initial reactions of the isoprene oxidation scheme in MECCA are given in Table 5.

The ratio of observation to model results for both OH and HO₂ as a function of the mixing ratio of isoprene is indeed clearly correlated, as shown in Fig. 12. For isoprene mixing ratios below 200 pptV, the ratios of observation to model concentrations vary around 1.37 ± 0.38 for OH and 0.98 ± 0.37 for HO₂, whereas for mixing ratios greater than 200 pptV the model increasingly underestimates the HO_x concentrations by more than a factor of 2. Dividing into isoprene logarithmic bins of $\Delta \ln x = 0.5$, x : isoprene mixing ratio, leads to maximum observed to modelled ratios of

HO_x over the tropical rainforest: box model results

D. Kubistin et al.

Title Page

Abstract

Introduction

Conclusions

References

Tables

Figures

◀

▶

◀

▶

Back

Close

Full Screen / Esc

Printer-friendly Version

Interactive Discussion



13±2 (OH) and 3.7±0.8 (HO₂) for the highest isoprene mixing ratios of 5.6±0.4 ppbV. A similar observation was made by Ren et al. (2008), who measured HO_x over a forest in the northern mid-latitudes. Their photochemical box model (Crawford et al., 1999) overestimated OH for isoprene mixing ratios lower than 500 pptV, and increasingly underestimated the concentrations for isoprene levels exceeding 500 pptV. Although the absolute values differ from the GABRIEL studies, the performance of both models shows a similar tendency with respect to isoprene. The coincidence of the qualitative behaviour of the two different box models for different field campaigns points either to a more fundamental gap in our knowledge of the isoprene degradation mechanism or to missing sources of OH with the same emission behaviour as isoprene.

4.2 Simulation with the Master Chemical Mechanism MCM

To test the performance of the lumped mechanism MIM, the more detailed isoprene chemistry of the MCM (Pinho et al., 2005) was included in the box model MECCA for comparison. More species (213 in total) were taken into account and the reaction scheme included several additional photolytic reactions. As the absorption cross sections and the quantum yields were not available for all implemented species, the photolysis frequencies (J) could not be calculated with the TUV model. Therefore, photolysis frequencies for species for which this information was available were used for all species of similar chemical structure as grouped in the MCM. The resulting photolysis frequencies are very uncertain, therefore sensitivity studies concerning the photolytic reactions were performed by varying the J-values by a factor of 10⁻³ and 10³. In order to avoid possible overestimation of H₂O₂, only the datasets with measured peroxide data available were taken into account. In Table 6, the photolytic reactions with the strongest effect on OH (more than 10% compared to the base run) are listed. The photolysis frequencies of the two isomers of the isoprene peroxy radical (2-hydroperoxy-2-methylbut-3-en-1-ol (ISOPBOOH) and 2-hydroperoxy-3-methylbut-3-en-1-ol (ISOPDOOH)) were the most prominent. As recommended in the MCM, the photolysis frequency of CH₃OOH was used for the analysis, calculated with the absorption cross

HO_x over the tropical rainforest: box model results

D. Kubistin et al.

Title Page

Abstract

Introduction

Conclusions

References

Tables

Figures

◀

▶

◀

▶

Back

Close

Full Screen / Esc

Printer-friendly Version

Interactive Discussion



section given by Vaghjiani and Ravishankara (1989) with quantum yields of unity. Increasing this photolysis frequency by a factor of 10^3 enhanced OH and HO₂ concentrations by 24%. Reduction of any of these frequencies by a factor of 10^{-3} led to a maximum reduction of 2% in OH. Thus, photolysis reactions in the model with unknown photolysis frequencies, with respect to OH and HO₂, were not relevant unless the photolysis frequencies were very strongly underestimated.

Variation of the photolysis of methacrolein (MACR) has a strong impact on OH. However, the absorption cross sections for methylvinylketone (MVK) and MACR have been measured (Gierczak et al., 1997). The variation of a factor 10^3 was unrealistically high but emphasizes the effect of the photolysis products. Increasing the photolysis frequency of MACR by 10^3 led to a large underestimation of OH (Table 6), indicating that the products deplete OH in further reactions.

During GABRIEL only the total sum of MVK and MACR was measured. For the studies with the MCM mechanism, these two species are treated separately. A ratio of MVK:MACR=2:1 was used (Kuhn et al., 2007). Simulations with ratios of MVK:MACR=0:1 and 1:0 changed the OH concentration about -5% and +3%, the HO₂ concentration +20% and -10%, respectively. In MIM the two species are lumped together.

Although 493 more explicit reactions were considered in the extensive isoprene chemistry scheme of the MCM, similar results were obtained as for the lumped mechanism MIM (Fig. 12). The reduced chemical mechanism of MIM was developed on the basis of the MCM (Poeschl et al., 2000) and the results in Fig. 12 confirm that the MIM performs well within the original objective. Neither the simplification of the MIM chemistry nor the assumptions made for the MCM simulations explained the discrepancies between models and observations. Possible explanations might lead to more fundamental chemistry (D. Taraborrelli, personal communication, 2008) or e.g. to segregation effects (Butler et al., 2008).

HO_x over the tropical rainforest: box model results

D. Kubistin et al.

Title Page

Abstract

Introduction

Conclusions

References

Tables

Figures

◀

▶

◀

▶

Back

Close

Full Screen / Esc

Printer-friendly Version

Interactive Discussion



4.3 Testing the HO_x cycling mechanism in MECCA

The HO_x cycling mechanisms are illustrated in Fig. 13. In the remote troposphere OH is converted to HO₂ mainly via carbon monoxide and recycled from HO₂ by reactions with nitric oxide and ozone. However over the rainforest, OH is removed by reactions with the emitted VOC, producing peroxy radicals. These peroxy radicals react either with other peroxy radicals or NO forming HO₂, or with HO₂ producing peroxides. Total radical loss from the radical cycle occurs by removing OH, RO₂ and HO₂ from the system. One major loss pathway over the rainforest is the formation of organic peroxides. Although the photolysis of peroxides is also a source of radicals, this channel is minor compared to the radical production via photolysis of ozone and reaction with water vapour, or the photolysis of HCHO. Organic peroxides are also removed from the system by dry deposition (Stickler et al., 2007).

One possible reason for the underestimation of OH and HO₂ in the model is an overestimation of modelled radical removal through the production of organic peroxides, especially the peroxides of isoprene and MACR+MVK (ISOOH, MVKOOH). For isoprene mixing ratios >2 ppbV, which are typical for the afternoon over the rainforest at altitudes <1 km, about 50% of all RO₂ form ROOH, the other 50% forming HO₂ (branching ratio: (RO₂→ROOH)/(RO₂→HO₂+HCHO)=1.03±0.22). Since photolysis of organic peroxides is negligible for radical production, the sensitivity of HO_x to the reaction rate of HO₂ with RO₂ can be investigated by taking these reactions out of the model. For the HO₂ concentration this modified simulation leads to an enhancement factor of 2.5±0.2 at maximum isoprene mixing ratios of (5.6±0.4) ppbV, improving the comparison with the observation. However the influence on OH is small, leading to an increase only by a factor of 1.2±0.1.

By constraining the HO₂ concentration to the observations, OH increases only by a factor of 1.7±0.2. Thus the enhancement of HO₂ in the model does not imply an increase of OH sufficient to describe the observations, which instead requires additional recycling from HO₂ to OH in the model or additional direct sources for OH, as also

HO_x over the tropical rainforest: box model results

D. Kubistin et al.

Title Page

Abstract

Introduction

Conclusions

References

Tables

Figures

◀

▶

◀

▶

Back

Close

Full Screen / Esc

Printer-friendly Version

Interactive Discussion



proposed by Tan et al. (2001).

An additional OH recycling reaction, $\text{HO}_2 + \text{X} \rightarrow \text{OH} + \text{X}'$, is a possible pathway to increase the simulated OH concentration. According to Hasson et al. (2004), certain alkyl peroxy radicals react with HO_2 yielding OH (Reaction R8):



Such reactions would also decrease the organic peroxides which were overestimated by MECCA for GABRIEL (Stickler et al., 2007). Hasson et al. (2004) examined the additional Reaction (R8) for ethyl peroxy ($\text{C}_2\text{H}_5\text{O}_2$), acetyl peroxy ($\text{CH}_3\text{C}(\text{O})\text{O}_2$) and acetonyl peroxy ($\text{CH}_3\text{C}(\text{O})\text{CH}_2\text{O}_2$) radicals, finding a yield of 40% for acetyl peroxy radicals. Further studies concerning this type of reaction by Dillon and Crowley (2008) and Jenkin et al. (2007) showed similar results and typical yields of about 50% or higher. To assess the effect of this additional OH recycling, all RO_2 reactions with HO_2 were modified in MECCA without distinction between different species. The branching ratio was varied between 50% and 90%, the latter obviously an upper limit. Nevertheless, even for the largest branching ratio the observed OH concentrations are still not reproduced. For the highest observed isoprene mixing ratios of (5.6 ± 0.4) ppbV the modification of MECCA produces maximum factors of 1.42 ± 0.04 and 2.42 ± 0.24 more OH for yields of 50% and 90% compared to the base runs (Fig. 14). This effect is still too small compared to the factors up to 13 needed to reproduce the measured OH concentrations under conditions of high isoprene. For HO_2 similar enhancement factors are obtained with 1.35 ± 0.06 and 1.99 ± 0.21 for the two OH yields, while factors of 3.7 are needed to reproduce the observations.

Another possible source of OH is the photolysis of organic peroxy radicals by near-infrared radiation via intramolecular rearrangement producing OH or HO_2 (Frost et al.,

HO_x over the tropical rainforest: box model results

D. Kubistin et al.

Title Page

Abstract

Introduction

Conclusions

References

Tables

Figures

◀

▶

◀

▶

Back

Close

Full Screen / Esc

Printer-friendly Version

Interactive Discussion



1999):



The photolysis frequency was assumed to follow that of NO_3 with values of 10^{-3} to 10^{-1} times $J(\text{NO}_3)$. The additional photochemical reactions were implemented in the model for all RO_2 to produce 100% OH via Reaction (R9), while no reaction channel to produce HO_2 was included. The highest photolysis frequency was chosen for the simulation shown here to obtain an upper limit (Fig. 14). For isoprene mixing ratios of (5.6 ± 0.4) ppbV the model with the additional chemistry leads to enhancement factors of 2.65 ± 0.56 for OH and 1.08 ± 0.02 for HO_2 compared to the base run. This is again insufficient to reproduce the observed HO_x concentrations, even though the results represent an upper limit.

None of the proposed reaction amendments alone is sufficient to reproduce the measured data in the model. As a further step, both OH recycling reaction of RO_2 with HO_2 and infrared photolysis of RO_2 were included in the model reaction scheme with maximum yields for OH (90% yield for Reaction R8 and $10^{-1} \cdot J(\text{NO}_3)$ for Reaction R9). Even then, simulated HO_x remains too low with enhancement factors of 5.1 ± 1.1 for OH and 2.1 ± 0.2 for HO_2 .

Ozonolysis of monoterpenes can also be an OH source (Tan et al., 2001) and is not considered in the model. As monoterpene emissions show a similar diurnal dependence as those of isoprene (Williams et al., 2007) their contribution to the OH concentration over the rainforest would be strongest in the afternoon. For the GABRIEL campaign α - and β -pinene were measured with maximum mixing ratios of the order of 200 pptV. Ozonolysis of monoterpenes was estimated to be about $10^5 \text{ molec cm}^{-3} \text{ s}^{-1}$ (Atkinson et al., 2005) over the rainforest in the afternoon, which is negligible compared to the primary production term (R1) of $3 \times 10^6 \text{ molec cm}^{-3} \text{ s}^{-1}$. The influence of monoterpenes and sesquiterpenes has been studied in detail by Ganzeveld et al. (2008), who compared the GABRIEL data with a single-column model, also concluding

HO_x over the tropical rainforest: box model results

D. Kubistin et al.

Title Page

Abstract

Introduction

Conclusions

References

Tables

Figures

◀

▶

◀

▶

Back

Close

Full Screen / Esc

Printer-friendly Version

Interactive Discussion

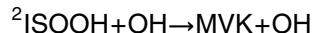


that ozonolysis of these species does not eliminate the large discrepancies between modelled and observed OH.

4.4 HO_x budget

An overview of the most relevant reactions for the HO_x budget in MECCA is given in Tables 7 and 8 to identify the main processes of the production and loss terms of OH and HO₂ for four groups of data. Case 1 is based on observations in the boundary layer over the rainforest, at altitudes lower than 1 km, in the morning (08:00–11:00 LT). Data from the same location in the afternoon (14:00–17:00 LT) are analysed in the second group. Data from the free troposphere over the ocean at an altitude of 2–4 km around noon (11:00–14:00 LT) are used for case 3, and data collected over the rainforest in the afternoon at the same altitude for case 4. Only the cases with at least 6 data points are discussed. Data at altitudes higher than 4 km are not considered, owing to the unavailability of measurements of peroxides, which become important for HO_x chemistry as H₂O concentrations decrease.

The primary production of OH in the lower troposphere is the photolysis of ozone followed by reaction with water vapour. Primary production rates are of the order of 40%–60% of the total production. The NO mixing ratios are highest in the morning boundary layer over the forest with (65±57) pptV, compared to (13±9) pptV, (10±3) pptV and (8±4) pptV for the other three cases, respectively. In the morning, solar radiation is still low and the OH radical recycling by reaction NO+HO₂ is comparable with the primary OH source. For all other cases the OH recycling via reaction of HO₂ is weak compared to the primary production. As the emissions of BVOCs increase during daytime, these compounds and their oxidation products increasingly influence the OH chemistry. The recycling of OH via the reactions of isoprene peroxides ISOOH+OH² in MIM is one of the major conversion mechanisms in MECCA and illustrates their importance to the chemistry of isoprene. The loss of OH in the boundary layer, according to MECCA, is



HO_x over the tropical rainforest: box model results

D. Kubistin et al.

Title Page

Abstract

Introduction

Conclusions

References

Tables

Figures

◀

▶

◀

▶

Back

Close

Full Screen / Esc

Printer-friendly Version

Interactive Discussion



dominated by the reaction with isoprene. As isoprene concentrations increase during the day, the proportion of this reaction with respect to the total loss increases to 62% in the afternoon and is even more important than the primary production term (53%). When less isoprene is available, the removal of OH by CO and peroxides becomes more significant.

The recycling reactions of $\text{RO}_2 + \text{NO}$ are the dominant processes for HO_2 production in the morning boundary layer over the forest (case 1), when NO concentrations are relatively high. When irradiation increases, photolysis of formaldehyde becomes an important source of the HO_2 radical (case 2). In the free troposphere the main source of HO_2 is the reaction of OH with carbon monoxide. Recycling of OH by the reaction $\text{NO} + \text{HO}_2$ dominates the loss of HO_2 when morning NO is high within the forest boundary layer, initially not leading to radical loss. For the remaining cases the reaction with peroxy radicals and the self reaction, producing peroxides, are the major loss terms for HO_2 . Since the photolysis of peroxides is slow to produce radicals, the production of peroxides effectively leads to removal of two radicals per reaction from the system.

Interconversion of HO_2 and OH via reactions with e.g. NO, O_3 , CO and VOC (Fig. 13) can be characterized by the chain length of the reactions cycling between these two radicals. The HO_2/OH ratio in the forest boundary layer in the morning (case 1) shows a mean value of 127 ± 34 at mean NO mixing ratios of (65 ± 57) pptV. The value is comparable to results from Tan et al. (2001), who found HO_2/OH ratios of 80–120 for mean NO levels of 65.8 pptV over deciduous forest in northern latitudes. Simulation by MECCA slightly overestimates the ratio with $\text{HO}_2/\text{OH} = 156 \pm 45$. For the forest boundary layer in the afternoon (case 2) values of $\text{HO}_2/\text{OH} = 234 \pm 44$ were observed for mean NO mixing ratios of (13 ± 9) pptV. The model overestimates this ratio of HO_2 to OH by a factor of 3.2 ± 0.8 , OH being underestimated more severely than HO_2 in the simulations. However, the correlation with the isoprene mixing ratio observed for OH and HO_2 (Fig. 12) is not significant for the ratio (Fig. 15) since the effect of isoprene on OH and HO_2 is similar for both radicals. The analysis of the different reactions relevant for the HO_x budget (Table 7) shows that isoprene and its peroxy radicals are the major compounds

HO_x over the tropical rainforest: box model results

D. Kubistin et al.

Title Page

Abstract

Introduction

Conclusions

References

Tables

Figures

◀

▶

◀

▶

Back

Close

Full Screen / Esc

Printer-friendly Version

Interactive Discussion



responsible for HO_x loss (~50%) in the afternoon forest boundary layer. OH is directly removed by reaction with isoprene, producing the peroxy radical ISO₂, which either removes HO₂ from the system, forming the peroxide ISOOH (60%), or produces HO₂ and formaldehyde by reactions with RO₂ or NO (40%).

5 4.5 Recycling probability and missing source strength for OH

To determine the recycling strength of the chemical system, the recycling probability has been calculated. The OH recycling probability r is defined as (Lelieveld et al., 2002):

$$r = \frac{S}{P + S}, \quad (1)$$

with P and S being the primary and secondary production, respectively. The primary production is considered to be only the reaction of O(¹D)+H₂O, whereas photolysis of peroxides and recycling reactions of HO₂ are assumed to be secondary productions terms, as the reactants are oxidation products in the OH oxidation chain. The base simulation of MECCA yields $P=3.12 \times 10^6$ molec cm⁻³ s⁻¹ and $S=1.94 \times 10^6$ molec cm⁻³ s⁻¹ and therefore $r=0.38$ for boundary layer values over the forest in the afternoon (case 2). The total loss term L in steady state simulations is equal to the total production term G with $L=G=P+S=5.06 \times 10^6$ molec cm⁻³ s⁻¹. Calculations using measured higher OH and HO₂ with the same chemical mechanism leads to $P=3.12 \times 10^6$ molec cm⁻³ s⁻¹ and $S=3.53 \times 10^6$ molec cm⁻³ s⁻¹. The total production term is therefore $G=6.65 \times 10^6$ molec cm⁻³ s⁻¹ compared to the total loss term of $L=56.64 \times 10^6$ molec cm⁻³ s⁻¹, calculated with MECCA for the HO_x observations. Thus, a production rate term of the order $S^*=5 \times 10^7$ molec cm⁻³ s⁻¹ is missing. Adding the missing term as secondary production would lead to a recycling probability due to the observation of $r=0.94$. Considering that this value of r is very high, it may be speculated that part of the missing OH formation is related to primary formation involving O₃. Previously it has been indicated that reactions of O₃ with reactive terpenes might be

HO_x over the tropical rainforest: box model results

D. Kubistin et al.

Title Page

Abstract

Introduction

Conclusions

References

Tables

Figures

◀

▶

◀

▶

Back

Close

Full Screen / Esc

Printer-friendly Version

Interactive Discussion



important (Tan et al., 2001; Di Carlo et al., 2004; Goldstein et al., 2004). Alternatively, O_3 may react with reaction products in the isoprene degradation pathway, produce OH and reduce the discrepancy, which would moderate the OH recycling probability.

The missing term S^* is comparable to the loss rate due to isoprene. By neglecting the entire isoprene chemistry in the box model MECCA, good agreement between simulations and HO_x observations is obtained, independently of the isoprene concentrations that were observed (Fig. 16). This indicates that the reason for the model underestimations rather lies in the oxidation mechanism of isoprene than in missing direct sources. An observed to modelled ratio of 1.26 ± 0.48 for OH is found for all measured isoprene mixing ratios. The situation for HO_2 is somewhat different. For low isoprene (<200 pptV) the model now tends to overestimate HO_2 , but is still well described within the uncertainty (0.86 ± 0.32). In contrast to OH, the dependence on the isoprene concentration is still discernable, though small, possibly indicating an additional influence on HO_2 by other trace gases also dependent on the time of day.

Butler et al. (2008) analysed the GABRIEL dataset using a global model. Analogous to the implementations of Reaction (R8) in our model, they introduced a modification of the reaction of the isoprene peroxy radical ISO_2 with HO_2 producing n -OH in their reaction scheme:



An optimum number of $n=2$ was derived to best reproduce the OH observations. For our constrained box model the best agreement between observation and simulation was found for $n=3.2$ (Fig. 17). A mean measured to modelled ratio of 0.99 ± 0.25 was obtained for OH and the dependence on isoprene disappeared.

Reaction (R11) should be understood as a proxy for additional recycling within the isoprene chemistry. The equivalent reaction:



with best agreement for $m=1.3$ shows that regarding the initial step in the oxidation mechanism more OH has to be produced than destroyed. A mean value for the ob-

HO_x over the tropical rainforest: box model results

D. Kubistin et al.

Title Page

Abstract

Introduction

Conclusions

References

Tables

Figures

◀

▶

◀

▶

Back

Close

Full Screen / Esc

Printer-friendly Version

Interactive Discussion



served to model ratio of 1.37 ± 0.52 was calculated (Fig. 17). Additional sources of OH, comparable and correlated to the isoprene sink are needed to describe the observations. Unknown OH recycling within the isoprene oxidation mechanism seems the most likely way to provide the additional OH source, leading to a much larger oxidation capacity of the atmosphere over the tropical rainforest.

5 Conclusions

Higher HO_x concentrations over the tropical rainforest during the GABRIEL campaign were observed than predicted by the box model MECCA constrained by measurements. Observations and simulations agree fairly well for the free troposphere, whereas maximum deviations were found for low altitudes (<1 km) in the afternoon with mean discrepancy factors of 12.2 ± 3.5 and 4.1 ± 1.4 for OH and HO_2 , respectively. These discrepancies are strongly correlated to isoprene emitted by the rainforest. However, the OH/ HO_2 ratio does not show a significant dependence on isoprene, as OH and HO_2 are similarly influenced by isoprene. Simulations with the more detailed isoprene mechanism of the MCM leads to similar results as the MIM chemical reaction scheme, indicating that the original objective of using a condensed mechanism to reproduce the results of the MCM is still met.

Radical loss from the system via removal of RO_2 producing organic peroxides, appears to be about 50% for air in the afternoon boundary layer. Sensitivity studies eliminating the production of organic peroxides increase the HO_2 and OH concentrations, but not sufficiently to achieve agreement with the observations.

Enhancement of photolysis frequencies of organic peroxides by unlikely factors of 10^3 do not provide a sufficient source for HO_x . Constraining the model to measured HO_2 enhances OH, but is also insufficient to match observations. Therefore, an additional production channel of OH is needed to explain the OH observed over the rainforest. Modification of the chemistry scheme of MECCA could not sufficiently enhance the the simulated HO_x concentration, either by recycling of OH through reaction of peroxy

HO_x over the tropical rainforest: box model results

D. Kubistin et al.

Title Page

Abstract

Introduction

Conclusions

References

Tables

Figures

◀

▶

◀

▶

Back

Close

Full Screen / Esc

Printer-friendly Version

Interactive Discussion



radicals with HO₂ or through infrared photolysis of peroxy radicals, or by combining the two.

The major OH and HO₂ sources over the rainforest (<1 km) in the afternoon are the reaction of O(¹D)+H₂O and the photolysis of HCHO. When available in the atmosphere, isoprene and its oxidation products strongly influence the OH chemistry leading to a loss rate of OH in the model comparable to the primary production rate. A recycling probability of $r=0.38$ follows from the standard simulation, whereas a value of up to $r=0.94$ is needed to explain the observations. An OH source stronger than the loss rate owing to ISOP+OH is evidently missing in the chemical mechanism based on current understanding ($S^*=5\times 10^7 \text{ molec cm}^{-3} \text{ s}^{-1}$). By neglecting the isoprene chemistry in MECCA, the underestimation of the HO_x simulations disappears. This leads to the hypothesis that the recycling of OH, mainly in the isoprene oxidation mechanism, is more efficient than predicted by the current reaction schemes. The additional recycling reaction via ISOP+OH→ISO₂+ m ·OH with $m=1.3$ improves the agreement with the OH observations, and further investigations to unravel the detailed chemical mechanisms are recommended.

Acknowledgements. The authors are grateful to the whole GABRIEL team, ENVISCOPE GmbH (Frankfurt, Germany) and GFD (Hohn, Germany) for their support, essential for the successful realisation of the GABRIEL campaign. We appreciate the good cooperation with the Suriname Meteorological Service (MDS) and the Anton de Kom University of Suriname (both in Paramaribo, Suriname).



MAX-PLANCK-GESELLSCHAFT

The publication of this article is
financed by the Max Planck Society.

15258

ACPD

8, 15239–15289, 2008

HO_x over the tropical rainforest: box model results

D. Kubistin et al.

Title Page

Abstract

Introduction

Conclusions

References

Tables

Figures

◀

▶

◀

▶

Back

Close

Full Screen / Esc

Printer-friendly Version

Interactive Discussion



References

- Atkinson, R., Baulch, D. L., Cox, R. A., Crowley, J. N., Hampson, R. F., Hynes, R. G., Jenkin, M. E., Rossi, M. J., and Troe, J.: Evaluated kinetic and photochemical data for atmospheric chemistry: Volume I – gas phase reactions of O_x, HO_x, NO_x and SO_x species, *Atmos. Chem. Phys.*, 4, 1461–1738, 2004,
5 <http://www.atmos-chem-phys.net/4/1461/2004/>. 15244
- Atkinson, R., Baulch, D. L., Cox, R. A., Crowley, J. N., Hampson, R. F., Hynes, R. G., Jenkin, M. E., Rossi, M. J., and Troe, J.: Evaluated kinetic and photochemical data for atmospheric chemistry: Volume II – reactions of organic species, *Atmos. Chem. Phys.*, 6, 3625–4055, 10 2006,
<http://www.atmos-chem-phys.net/6/3625/2006/>. 15244, 15252
- Butler, T. M., Taraborrelli, D., Brühl, C., Fischer, H., Harder, H., Martinez, M., Williams, J., Lawrence, M. G., and Lelieveld, J.: Improved simulation of isoprene oxidation chemistry with the ECHAM5/MESy chemistry-climate model: lessons from the GABRIEL airborne field
15 campaign, *Atmos. Chem. Phys. Discuss.*, 8, 6273–6312, 2008,
<http://www.atmos-chem-phys-discuss.net/8/6273/2008/>. 15249, 15256
- Crawford, J., Davis, D., Olson, J., Chen, G., Liu, S., Gregory, G., Barrick, J., Sachse, G., Sandholm, S., Heikes, B., Singh, H., and Blake, D.: Assessment of upper tropospheric HO_x source over the tropical Pacific based on NASA GTE/PEM data: Net affect on HO_x and other
20 photochemical parameters, *J. Geophys. Res.*, 104, 16 255–16 273, 1999. 15248
- Di Carlo, P., Brune, W. H., Martinez, M., Harder, H., Leshner, R., Ren, X. Thornberry, T., Carroll, M. A., Young, V., Shepson, P. B., Riemer, D., Apel, E. and Campbell, C.: Missing OH Reactivity in a Forest: Evidence for Unknown Reactive Biogenic VOCs, *Science*, 304, 722–725, 2004. 15256
- 25 Dillon, T. J. and Crowley, J. N.: Direct detection of OH formation in the reactions of HO₂ with CH₃C(O)O₂ and other substituted peroxy radicals, *Atmos. Chem. Phys. Discuss.*, 8, 7111–7146, 2008,
<http://www.atmos-chem-phys-discuss.net/8/7111/2008/>. 15251
- Eerdeken, G., Ganzeveld, L., Vilà-Guerau de Arellano, J., Klüpfel, T., Sinha, V., Yassaa, N., Williams, J., Harder, H., Kubistin, D., Martinez, M., and Lelieveld, J.: Flux estimates of isoprene, methanol and acetone from airborne PTRMS measurements over the tropical rainforest during the GABRIEL 2005 campaign, *Atmos. Chem. Phys. Discuss.*, 8, 12 903–12 969,
- 30

ACPD

8, 15239–15289, 2008

HO_x over the tropical rainforest: box model results

D. Kubistin et al.

Title Page

Abstract

Introduction

Conclusions

References

Tables

Figures

◀

▶

◀

▶

Back

Close

Full Screen / Esc

Printer-friendly Version

Interactive Discussion



2008. 15247, 15266

Eisele, F. L., Mount, G. H., Fehsenfeld, F. C., Harder, J., Marovich, E., Parrish, D. D., Roberts, J., and Trainer, M.: Intercomparison of tropospheric OH and ancillary trace gas measurements at Fritz Peak Observatory, Colorado, *J. Geophys. Res.*, 99(18), 605–626, 1994. 15242

5 Fehsenfeld, F., Calvert, J., Fall, R., Goldan, P., Guenther, A. B., Hewitt, C. N., Lamb, B., Liu, S., Trainer, M., Westberg, H., and Zimmermann, P.: Emissions of volatile organic compounds from vegetation and the implications for atmospheric chemistry, *Global Biogeochem. Cycles*, 6, 389–430, 1992. 15241

10 Frost, G. J., Ellison, G. B., and Vaida, V.: Organic Peroxyl Radical Photolysis in the Near-Infrared: Effects on Tropospheric Chemistry, *J. Phys. Chem. A*, 103, 10 169–10 178, 1999. 15251

Fuentes, J. D., Lerdau, M., Atkinson, R., et al.: Biogenic hydrocarbons in the atmospheric boundary layer: A review, *B. Am. Meteorol. Soc.*, 81(7), 1537–1575, 2000. 15241, 15243

15 Ganzeveld, L., Eerdekens, G., Feig, G., Fischer, H., Harder, H., Königstedt, R., Kubistin, D., Martinez, M., Meixner, F., Scheeren, B., Williams, J., and Lelieveld, J.: Surface and boundary layer exchanges of volatile organic compounds, nitrogen oxides and ozone during the GABRIEL Campaign, *Atmos. Chem. Phys. Discuss.*, 8, 11 909–11 965, 2008. 15252

20 Gierczak, T., Burkholder, J. B., Talukdar, R. K., Mellouki, A., Barone, S. B., and Ravishankara, A. R.: Atmospheric fate of methyl vinyl ketone and methacrolein, *J. Photochem. Photobiol. A: Chemistry*, 110, 1–10, 1997. 15249

Goldstein, A. H., McKay, M., Kurpius, M. R., Schade, G. W., Lee, A., Holzinger, R., and Rasmussen, R. A.: Forest thinning experiment confirms ozone deposition to forest canopy is dominated by reaction with biogenic VOCs, *Geophys. Res. Lett.*, 31, L22106, doi:10.1029/2004GL021259, 2004. 15256

25 Granier, C., Pétron, G., Müller, J.-F., and Brasseur, G.: The impact of natural and anthropogenic hydrocarbons on the tropospheric budget of carbon monoxide, *Atmos. Environ.*, 34, 5255–5270, 2000. 15242, 15247

Guenther, A. B., Hewitt, G. N., Erickson, D., et al.: A global model of natural volatile organic compound emissions, *J. Geophys. Res.*, 100(D5), 8873–8892, 1995. 15241, 15242, 15247

30 Hasson, A. S., Tyndall, G. S., and Orlando, J. J.: A product yield study of the reaction of HO₂ radicals with Ethyl Peroxy (C₂H₅O₂), Acetyl Peroxy (CH₃C(O)O₂), and Acetonyl Peroxy (CH₃C(O)CH₂O₂) Radicals, *J. Phys. Chem. A*, 108, 5979–5989, 2004. 15251

Heard, D. E. and Pilling, M. J.: Measurement of OH and HO₂ in the Troposphere, *Chem. Rev.*,

ACPD

8, 15239–15289, 2008

HO_x over the tropical rainforest: box model results

D. Kubistin et al.

Title Page

Abstract

Introduction

Conclusions

References

Tables

Figures

◀

▶

◀

▶

Back

Close

Full Screen / Esc

Printer-friendly Version

Interactive Discussion



103, 5163–5198, 2003. 15241

Jackson, A. V. and Hewitt, C. N.: Atmosphere Hydrogen Peroxide and Organic Hydroperoxides: A Review, *Crit. Rev. Environ. Sci. Technol.*, 29(2), 175–228, 1999. 15245

Jenkin, M. E. and Hayman, G. D.: Kinetics of Reactions of Primary, Secondary and Tertiary β -Hydroxy Peroxyl Radicals, Application to Isoprene Degradation, *J. Chem. Soc. Faraday Trans.*, 91(13), 1911–1922, 1995. 15242

Jenkin, M. E., Saunders, S. M., and Pilling, M. J.: The tropospheric degradation of volatile organic compounds: a protocol for mechanism development, *Atmos. Environ.*, 31, 81–104, 1997. 15242, 15244

Jenkin, M. E., Hurley, M. D., and Wallington, T. J.: Investigation of the radical product channel of the $\text{CH}_3\text{COO}_2 + \text{HO}_2$ reaction in the gas phase, *Phys. Chem. Chem. Phys.*, 9, 3149–3162, 2007. 15251

Jöckel, P., Tost, H., Pozzer, A., Brühl, C., Buchholz, J., Ganzeveld, L., Hoor, P., Kerweg, A., Lawrence, M. G., Sander, R., Steil, B., Stiller, G., Tanarhte, M., Taraborrelli, D., van Aardenne, J., and Lelieveld, J.: The atmospheric chemistry general circulation model ECHAM5/MESSy1: consistent simulation of ozone from the surface to the mesosphere, *Atmos. Chem. Phys.*, 6, 5067–5104, 2006, <http://www.atmos-chem-phys.net/6/5067/2006/>. 15242

Karl, T., Guenther, A., Yokelson, R. J., Greenberg, J., Potosnak, M., Blake, D. R., and Artaxo, P.: The tropical forest and fire emissions experiment: Emission, chemistry and transport of biogenic volatile organic compounds in the lower atmosphere over Amazonia, *J. Geophys. Res.*, 112, D18302, doi:10.1029/2007JD008539, 2007. 15241

Kesselmeier, J. and Staudt, M.: Biogenic volatile organic compounds (VOC): An overview on emission, physiology and ecology, *J. Atmos. Chem.*, 33, 23–88, 1999. 15241

Von Kuhlmann, R., Lawrence, M. G., Pöschl, U., and Crutzen, P. J.: Sensitivities in global scale modelling of isoprene, *Atmos. Chem. Phys.* 4, 1–17, 2004. 15242

Kuhn, U., Andreae, M. O., Ammann, C., Araújo, A. C., Brancaleoni, E., Ciccioli, P., Dindorf, T., Frattoni, M., Gatti, L. V., Ganzeveld, L., Kruijt, B., Lelieveld, J., Lloyd, J., Meixner, F. X., Nobre, A. D., Pöschl, U., Spirig, C., Stefani, P., Thielmann, A., Valentini, R., and Kesselmeier, J.: Isoprene and monoterpene fluxes from Central Amazonian rainforest inferred from tower-based and airborne measurements, and implications on the atmospheric chemistry and the local carbon budget, *Atmos. Chem. Phys.*, 7, 2855–2879, 2007, <http://www.atmos-chem-phys.net/7/2855/2007/>. 15249

ACPD

8, 15239–15289, 2008

HO_x over the tropical rainforest: box model results

D. Kubistin et al.

Title Page

Abstract

Introduction

Conclusions

References

Tables

Figures

◀

▶

◀

▶

Back

Close

Full Screen / Esc

Printer-friendly Version

Interactive Discussion



HO_x over the tropical rainforest: box model results

D. Kubistin et al.

[Title Page](#)[Abstract](#)[Introduction](#)[Conclusions](#)[References](#)[Tables](#)[Figures](#)[◀](#)[▶](#)[◀](#)[▶](#)[Back](#)[Close](#)[Full Screen / Esc](#)[Printer-friendly Version](#)[Interactive Discussion](#)

- Lelieveld, J., Peters, V., Dentener, F. J., and Krol, M.: Stability of tropospheric hydroxyl chemistry, *J. Geophys. Res.*, 107, D23, doi:10.1029/2002JD002272, 2002. 15241, 15242, 15255
- Lelieveld, J., Butler, T. M., Crowley, J., Dillon, T., Fischer, H., Ganzeveld, L., Harder, H., Lawrence, M. G., Martinez, M., Taraborrelli, D., and Williams, J.: Atmospheric oxidation capacity sustained by a tropical forest, *Nature*, 452, 737–740, 2008. 15243
- Levy II, H.: Normal atmosphere: Large radical and formaldehyde concentrations predicted, *Science*, 173, 141–143, 1971. 15241
- Logan, J. A., Prather, M. J., Wofsy, S. C., and McElroy, M. B.: Tropospheric chemistry: A global perspective, *J. Geophys. Res.*, 86, 7210–7254, 1981. 15241
- Madronich, S. and Flocke, S.: The role of solar radiation in atmospheric chemistry, in: *Handbook of Environmental Chemistry*, edited by: Boule, P., pp. 1–26, Springer, New York, 1998. 15244
- Martinez, M., Harder, H., Kubistin, D., Rudolf, M., Bozem, H., Eerdeken, G., Fischer, H., Gurk, C., Königsstedt, R., Klüpfel, T., Parchatka, U., Schiller, C. L., Stickler, A., Williams, J., and Lelieveld, J.: Hydroxyl radicals in the tropical troposphere over the Suriname rainforest: airborne measurements, *Atmos. Chem. Phys. Discuss.*, accepted, 2008. 15243, 15266
- Paulson, S. E., Flagan, R. C., and Seinfeld, J. H.: Atmospheric photo-oxidation of isoprene: part I: the hydroxyl radical and ground state atomic oxygen reactions, *Int. J. Chem. Kin.*, 24, 79–101, 1992. 15242
- Pinho, P. G., Pio, C. A., and Jenkin, M. E.: Evaluation of isoprene degradation in the detailed tropospheric chemical mechanism, MCM v3, using environmental chamber data, *Atmos. Environ.*, 39, 1303–1322, 2005. 15248
- Pöschl, U., Von Kuhlmann, R., Poisson, N., and Crutzen, P. J.: Development and intercomparison of condensed isoprene oxidation mechanisms for global atmospheric modeling, *J. Atmos. Chem.*, 37, 29–52, 2000. 15244, 15249
- Poisson, N., Kanakidou, M., and Crutzen, P. J.: Impact of Non-Methane Hydrocarbons on Tropospheric Chemistry and the Oxidizing Power of the Global Troposphere: 3-Dimensional Modelling Results, *J. Atmos. Chem.*, 36, 157–230, 2000. 15242
- Ren, X., Olson, J. R., Crawford, J. H., Brune, W. H., Mao, J., Long, R. B., Chen, Z., Chen, G., Avery, M. A., Sachse, G. W., Barrick, J. D., Diskin, G. S., Huey, L. G., Fried, A., Cohen, R. C., Heikes, B., Wennberg, P., Singh, H. B., Blake, D. R., and Shetter, R. E.: HO_x chemistry during INTEX-A 2004: Observation, model calculation, and comparison with previous studies, *J. Geophys. Res.*, 113, D05310, doi:10.1029/2007JD009166, 2008. 15248

- Sander, R., Kerkweg, A., Jöckel, P., and Lelieveld, J.: Technical note: The new comprehensive atmospheric chemistry module MECCA, *Atmos. Chem. Phys.*, 5, 445–450, 2005, <http://www.atmos-chem-phys.net/5/445/2005/>. 15244
- Sander, S. P., Friedl, R. R., Golden, D. M., Kurylo, M. J., Moortgat, G. K., Wine, P. H., Ravishankara, A. R., Kolb, C. E., Molina, M. J., Finlayson-Pitts, B. J., Huie, R. E., and Orkin, V. L.: Chemical Kinetics and Photochemical Data for Use in Atmospheric Studies, Evaluation Number 15, JPL Publication 06-2, NASA Jet Propulsion Laboratory, Pasadena, California, 2006. 15244
- Saunders, S. M., Jenkin, M. E., Derwent, R. G., and Pilling, M. J.: World wide web site of a master chemical mechanism (MCM) for use in tropospheric chemistry models, available at: <http://www.chem.leeds.ac.uk/Atmospheric/MCM>, *Atmos. Environ.*, 31, 1249, 1997. 15244
- Saunders, S. M., Jenkin, M. E., Derwent, R. G., and Pilling, M. J.: Protocol for the development of the Master Chemical Mechanism, MCM v3 (Part A): tropospheric degradation of non-aromatic volatile organic compounds, *Atmos. Chem. Phys.*, 3, 161–180, 2003, <http://www.atmos-chem-phys.net/3/161/2003/>. 15244
- Schmidt, U.: Molecular hydrogen in the atmosphere, *Tellus*, 26, 78–90, 1974. 15267
- Schmidt, U.: The latitudinal and vertical distribution of molecular hydrogen in the troposphere, *J. Geophys. Res.*, 83, 941–946, 1978. 15267
- Stickler A., Fischer, H., Bozem, H., Gurk, C., Schiller, C., Martinez-Harder, M., Kubistin, D., Harder, H., Williams, J., Eerdeken, G., Yassaa, N., Ganzeveld, L., Sander, R., and Lelieveld, J.: Chemistry, transport and dry deposition of trace gases in the boundary layer over the tropical Atlantic Ocean and the Guyanas during the GABRIEL field campaign, *Atmos. Chem. Phys.*, 7, 3933–3956, 2007, <http://www.atmos-chem-phys.net/7/3933/2007/>. 15245, 15250, 15251, 15266, 15267
- Tan., D., Faloon, I., Simpas, J. B., Brune, W., Shepson, P. B., Couch, T. L., Summer, A. L., Carroll, M. A., Thornberry, T., Apel, E., Riemer, D., and Stockwell, W.: HO_x budgets in a deciduous forest: Results from the PROPHET summer 1998 campaign, *J. Geophys. Res.*, 106, 24 407–24 427, 2001. 15251, 15252, 15254, 15256
- Vaghjiani, G. L. and Ravishankara, A. R.: Absorption cross sections of CH₃OOH, H₂O₂ and D₂O₂ vapors between 210 nm and 365 nm at 297 K, *J. Geophys. Res.*, 94, 3487–3492, 1989. 15249
- Wang, Y., Jacob, D. J., and Logan, J. A.: Global simulations of tropospheric O₃ – NO_x – hydrocarbon chemistry. 3 Origin of tropospheric ozone effects of non-methane hydrocarbons, *J.*

HO_x over the tropical rainforest: box model resultsD. Kubistin et al.

Title Page

Abstract

Introduction

Conclusions

References

Tables

Figures

◀

▶

◀

▶

Back

Close

Full Screen / Esc

Printer-friendly Version

Interactive Discussion



- Geophys. Res., 103, 10 757–10 767, 1998. 15242
- Warneke, C., Holzinger, R., Hansel, A., Jordan, A., Lindinger, W., Pöschl, U., Williams, J., Hoor, P., Fischer, H., Crutzen, P. J., Scheeren, H. A., and Lelieveld, J.: Isoprene and Its Oxidation Products Methyl Vinyl Ketone, Methacrolein, and Isoprene Related Peroxides Measured On-line over the Tropical Rain Forest of Suriname in March 1998, J. Atmos. Chem., 38, 167–185, 2001. 15247
- Williams, J., Yassaa, N., Bartenbach, S., and Lelieveld, J.: Mirror image hydrocarbons from Tropical and Boreal forests, Atmos. Chem. Phys., 7, 973–980, 2007, <http://www.atmos-chem-phys.net/7/973/2007/>. 15252
- 10 Zimmermann, P. R., Greenberg, J. P., and Westberg, C. E.: Measurements of atmospheric hydrocarbons and biogenic emission fluxes in the Amazon boundary layer, J. Geophys. Res., 93, 1407–1416, 1988. 15267

HO_x over the tropical rainforest: box model resultsD. Kubistin et al.

[Title Page](#)[Abstract](#)[Introduction](#)[Conclusions](#)[References](#)[Tables](#)[Figures](#)[I◀](#)[▶I](#)[◀](#)[▶](#)[Back](#)[Close](#)[Full Screen / Esc](#)[Printer-friendly Version](#)[Interactive Discussion](#)

HO_x over the tropical rainforest: box model results

D. Kubistin et al.

Table 1. Overview of flights performed during GABRIEL.

Flight	Date	Time of Day
G01	3 Oct 2005	afternoon
G02	5 Oct 2005	noon
G03	6 Oct 2005	afternoon
G04	7 Oct 2005	noon
G05	8 Oct 2005	noon
G06	10 Oct 2005	afternoon
G07	11 Oct 2005	morning
G08	12 Oct 2005	afternoon
G09	13 Oct 2005	afternoon
G10	15 Oct 2005	morning

[Title Page](#)[Abstract](#)[Introduction](#)[Conclusions](#)[References](#)[Tables](#)[Figures](#)[I◀](#)[▶I](#)[◀](#)[▶](#)[Back](#)[Close](#)[Full Screen / Esc](#)[Printer-friendly Version](#)[Interactive Discussion](#)

Table 2. Overview of the species observed and measurement techniques used during the GABRIEL campaign.

Species	Technique	not measured for flight
OH ^a	LIF ^b	G01
HO ₂ ^a	LIF	G01
J(NO ₂)	filter radiometry	
NO	chemiluminescence	G01, G05, G10
O ₃	chemiluminescence	G01
HCHO	QLAS ^c	G02
CO	QLAS	G02
ROOH ^{d,e}	derivatisation and fluorimetry	G01, (G05, G07)
H ₂ O ₂ ^e	derivatisation and fluorimetry	G01, G05, G07
Isoprene ^f	PTR-MS ^g	G01, G05
MVK+MACR ^{f,h}	PTR-MS	G01, G05
Acetone ^f	PTR-MS	G01, G05
Methanol ^f	PTR-MS	G01, G05
H ₂ O	LI-COR ⁱ	G02, G07

^a Martinez et al. (2008)

^b laser induced fluorescence

^c quantum cascade laser absorption spectroscopy

^d sum of organic peroxides

^e Stickler et al. (2007)

^f Eerdekens et al. (2008)

^g proton transfer reaction mass spectrometry

^h sum of methylvinylketones and methacrolein

ⁱ infrared absorption spectrometry

HO_x over the tropical rainforest: box model results

D. Kubistin et al.

Title Page

Abstract

Introduction

Conclusions

References

Tables

Figures

◀

▶

◀

▶

Back

Close

Full Screen / Esc

Printer-friendly Version

Interactive Discussion



HO_x over the tropical rainforest: box model results

D. Kubistin et al.

Table 3. Mixing ratios of species which were not measured during the GABRIEL campaign and were fixed for simulation ($\text{ppmV}=10^{-6} \frac{\text{mol}}{\text{mol}}$, $\text{ppbV}=10^{-9} \frac{\text{mol}}{\text{mol}}$, $\text{pptV}=10^{-12} \frac{\text{mol}}{\text{mol}}$). Mixing ratios of alkanes and alkenes were set to zero for altitudes >2 km, except for CH₄. Table taken from Stickler et al. (2007).

Species	Mixing ratio ≤2 km/>2 km	Reference
C ₂ H ₄	(650/0) pptV	GTE ABLE 2A, Manaus, Brazil (Zimmermann et al., 1988)
C ₂ H ₆	(794/0) pptV	LBA-CLAIRE98 campaign, IMAU (Univ. Utrecht, The Netherlands)
C ₃ H ₆	(83/0) pptV	LBA-CLAIRE98 campaign, IMAU (Univ. Utrecht, The Netherlands)
C ₃ H ₈	(83/0) pptV	LBA-CLAIRE98 campaign, IMAU (Univ. Utrecht, The Netherlands)
C ₄ H ₁₀	(28/0) pptV	LBA-CLAIRE98 campaign, IMAU (Univ. Utrecht, The Netherlands)
CH ₄	1.7 ppmV	NOAA CMDL Global Trends, ESRL Global Monitoring Division
CO ₂	377 ppmV	NOAA CMDL Global Trends, ESRL Global Monitoring Division
H ₂	563 ppbV	Schmidt (1974, 1978)
HNO ₃	0	

[Title Page](#)
[Abstract](#)
[Introduction](#)
[Conclusions](#)
[References](#)
[Tables](#)
[Figures](#)
[Back](#)
[Close](#)
[Full Screen / Esc](#)
[Printer-friendly Version](#)
[Interactive Discussion](#)


HO_x over the tropical rainforest: box model results

D. Kubistin et al.

Table 4. Sensitivity studies with MECCA concerning the constrained measured species. Concentrations are mean values for the forest boundary layer (<1 km) in the afternoon (14:00–17:00 LT).

	OH (molec/cm ³)	1 σ (%)	OH obs/mod	HO ₂ (molec/cm ³)	1 σ (%)	HO ₂ obs/mod
Observation	43.9×10 ⁵	21	1.0	10.2×10 ⁸	19	1.0
Reference Run	3.84×10 ⁵	32	12.2±3.5	2.63×10 ⁸	24	4.1±1.4
0.5 Isoprene	5.75×10 ⁵	31	8.1±2.2	2.78×10 ⁸	24	3.9±1.3
0.5 (MACR+MVK)	3.98×10 ⁵	31	11.8±3.4	2.64×10 ⁸	23	4.1±1.4
2 O ₃	6.24×10 ⁵	33	7.5±2.1	2.79×10 ⁸	24	3.9±1.4
2 NO	4.42×10 ⁵	32	10.7±3.4	2.90×10 ⁸	23	3.7±1.3
2 H ₂ O	5.55×10 ⁵	33	8.4±2.3	2.53×10 ⁸	24	4.3±1.5
0.5 CO	3.84×10 ⁵	33	12.2±3.5	2.58×10 ⁸	24	4.2±1.4
3 H ₂ O ₂	4.60×10 ⁵	37	10.5±3.2	2.73×10 ⁸	25	4.0±1.4
2 HCHO	3.96×10 ⁵	30	11.8±3.5	3.57×10 ⁸	25	3.1±1.1
0 Alkane	3.92×10 ⁵	32	11.9±3.4	2.63×10 ⁸	23	4.1±1.4
0.3 ROOH	3.74×10 ⁵	32	12.6±3.6	2.60×10 ⁸	23	4.2±1.4

Title Page

Abstract

Introduction

Conclusions

References

Tables

Figures

◀

▶

◀

▶

Back

Close

Full Screen / Esc

Printer-friendly Version

Interactive Discussion



HO_x over the tropical rainforest: box model results

D. Kubistin et al.

Title Page

Abstract

Introduction

Conclusions

References

Tables

Figures

◀

▶

◀

▶

Back

Close

Full Screen / Esc

Printer-friendly Version

Interactive Discussion



Table 5. Isoprene mechanism in MECCA. The entire chemical mechanism is described in the accompanying electronic supplement (<http://www.atmos-chem-phys-discuss.net/8/15239/2008/acpd-8-15239-2008-supplement.pdf>).

ISOP+O ₃	→	0.28 HCOOH+0.65 MVK+0.1 MVK ₂ +0.1 PA+0.14 CO+0.58 HCHO+0.09 H ₂ O ₂ + +0.08 CH ₃ O ₂ +0.25 OH+0.25 HO ₂ .	$k=7.86 \times 10^{-15} e^{-\frac{1913}{T}}$
ISOP+OH	→	ISO ₂ .	$k=2.54 \times 10^{-11} e^{-\frac{430}{T}}$
ISOP+NO ₃	→	ISON.	$k=3.03 \times 10^{-12} e^{-\frac{446}{T}}$
ISO ₂ +HO ₂	→	ISOOH.	$k=2.22 \times 10^{-13} e^{-\frac{1390}{T}}$
ISO ₂ +NO	→	0.956 NO ₂ +0.956 MVK+0.956 HCHO+0.956 HO ₂ +0.044 ISON.	$k=2.54 \times 10^{-12} e^{-\frac{360}{T}}$
ISO ₂ +CH ₃ O ₂	→	0.5 MVK+1.25 HCHO+HO ₂ +0.25 MGLO+0.25 ACETOL+ +0.25 CH ₃ OH.	$k=2.0 \times 10^{-12}$
ISO ₂ +ISO ₂	→	2 MVK+HCHO+HO ₂ .	$k=2.0 \times 10^{-12}$
ISOOH+OH	→	MVK+OH.	$k=1.0 \times 10^{-10}$
ISON+OH	→	ACETOL+NACA.	$k=1.3 \times 10^{-11}$
ISOOH+hν	→	MVK+HCHO+HO ₂ +OH	$J=J_{\text{CH}_3\text{OOH}}$
ISON+hν	→	MVK+HCHO+NO ₂ +HO ₂	$J=3.7 J_{\text{PAN}}$
MVK+O ₃	→	0.45 HCOOH+0.9 MGLO+0.1 PA+0.19 OH+0.22 CO+0.32 HO ₂ .	$k=0.5(1.36 \times 10^{-15} e^{-\frac{2112}{T}} + 7.51 \times 10^{-16} e^{-\frac{1521}{T}})$
MVK+OH	→	MVKO ₂ .	$k=0.5(4.1 \times 10^{-12} e^{-\frac{490}{T}} + 1.9 \times 10^{-11} e^{-\frac{176}{T}})$
MVKO ₂ +HO ₂	→	MVKOOH.	$k=1.82 \times 10^{-13} e^{-\frac{1390}{T}}$
MVKO ₂ +NO	→	NO ₂ +0.25 PA+0.25 ACETOL+0.75 HCHO+0.25 CO+0.75 HO ₂ +0.5 MGLO	$k=2.54 \times 10^{-12} e^{-\frac{360}{T}}$
MVKO ₂ +NO ₂	→	MPAN.	$k=0.25 k_{3rd}(T, M, 9.7 \times 10^{-29}, 5.6, 9.3 \times 10^{-12}, 1.5, 0.6)$
MVKO ₂ +CH ₃ O ₂	→	0.5 MGLO+0.375 ACETOL+0.125 PA+1.125 HCHO+0.875 HO ₂ +0.125 CO+ +0.25 CH ₃ OH.	$k=2.0 \times 10^{-12}$
MVKO ₂ +MVKO ₂	→	ACETOL+MGLO+0.5 CO+0.5 HCHO+ +HO ₂ .	$k=2.0 \times 10^{-12}$
MVKOOH+OH	→	MVKO ₂ .	$k=3.0 \times 10^{-12}$
MVK+hν	→	PA+HCHO+CO+HO ₂	$J=0.019 J_{\text{COH}_2} + 0.015 J_{\text{CH}_3\text{COCHO}}$
MVKOOH+hν	→	OH+0.5 MGLO+0.25 ACETOL+0.75 HCHO+0.75 HO ₂ +0.25 PA+0.25 CO	$J=J_{\text{CH}_3\text{OOH}}$

ISOP = isoprene, ISO₂ = isoprene (hydroxy) peroxy radicals, ISOOH = isoprene (hydro) peroxides, ISON = organic nitrates from ISO₂ and ISOP+NO₃,

MVK = methylvinylketone + methacrolein, MVK₂ = MVK / MACR peroxy radicals, MVKOOH = MVK / MACR hydroperoxides, MGLO = methylglyoxal,

PA = peroxy acetyl radical, NACA = nitro-oxy acetaldehyde, MPAN = peroxyacetyl nitrate + peroxyacetyl nitric anhydride, ACETOL = hydroxy acetone.

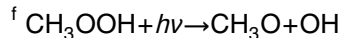
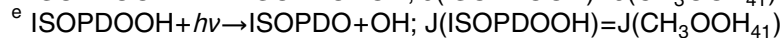
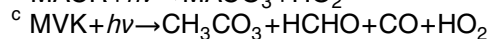
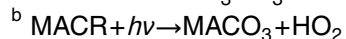
Reactions are taken from the MECCA v0.1p.

$$k_{3rd}(T, [M], k_0^{300}, n, k_\infty^{300}, m, f_c) = k_0(T) [M] \left(1 + \frac{k_0(T) [M]}{k_\infty(T)} \right)^{-1} f_c \left\{ 1 + \lg^2 \left(\frac{k_0(T) [M]}{k_\infty(T)} \right) \right\}^{-1},$$

$$k_0(T) = k_0^{300} \left(\frac{300}{T} \right)^n, k_\infty(T) = k_\infty^{300} \times \left(\frac{300}{T} \right)^m.$$

Table 6. Sensitivity studies of the photolysis frequencies concerning the isoprene chemistry of the MCM. Concentrations are mean values for the forest boundary layer (<1 km) in the afternoon (14:00–17:00 LT).

	OH (molec/cm ³)		OH obs/mod	HO ₂ (molec/cm ³)		HO ₂ obs/mod
		1 σ (%)			1 σ (%)	
Observation	43.9×10 ⁵	21	1.0	10.2×10 ⁸	19	1.0
Reference Run	3.71×10 ⁵	26	13.2±3.9	3.00×10 ⁸	23	3.8±1.3
10 ³ ·J(MACR ₁₈) ^a	2.48×10 ⁵	39	21.5±10.4	32.2×10 ⁸	21	0.4±0.1
10 ⁻³ ·J(MACR ₁₈)	3.67×10 ⁵	27	13.3±3.9	2.84×10 ⁸	24	4.0±1.4
10 ³ ·J(MACR ₁₉) ^b	0.17×10 ⁵	47	338±183	29.6×10 ⁸	21	0.4±0.1
10 ⁻³ ·J(MACR ₁₉)	3.71×10 ⁵	26	13.2±3.8	2.79×10 ⁸	24	3.9±1.4
10 ³ ·J(MVK ₂₄) ^c	4.48×10 ⁵	26	11.0±3.7	8.79×10 ⁸	22	1.3±0.5
10 ⁻³ ·J(MVK ₂₄)	3.71×10 ⁵	26	13.2±3.9	2.99×10 ⁸	23	3.8±1.3
10 ³ ·J(ISOPBOOH) ^d	4.62×10 ⁵	26	10.5±2.9	3.73×10 ⁸	21	3.0±1.0
10 ⁻³ ·J(ISOPBOOH)	3.68×10 ⁵	26	13.3±4.0	2.97×10 ⁸	24	3.8±1.3
10 ³ ·J(ISOPDOOH) ^e	4.16×10 ⁵	26	11.7±3.4	3.27×10 ⁸	23	3.5±1.2
10 ⁻³ ·J(ISOPDOOH)	3.70×10 ⁵	26	13.2±3.9	2.99×10 ⁸	23	3.8±1.3
10 ³ ·J(CH ₃ OOH ₄₁) ^f	4.06×10 ⁵	25	12.0±3.4	3.29×10 ⁸	22	3.4±1.1
10 ⁻³ ·J(CH ₃ OOH ₄₁)	3.70×10 ⁵	26	13.2±3.9	2.98×10 ⁸	24	3.8±1.3



HO_x over the tropical rainforest: box model results

D. Kubistin et al.

Title Page

Abstract

Introduction

Conclusions

References

Tables

Figures

◀

▶

◀

▶

Back

Close

Full Screen / Esc

Printer-friendly Version

Interactive Discussion



Table 7. OH budget based on a model analysis of measurement data.

	case 1: land morning BL 6 datapoints		case 2: land afternoon BL 23 datapoints		case 3: ocean noon (3.5±0.3) km 8 datapoints		case 4: land afternoon (3.3±0.4) km 20 datapoints	
production rate	$8.2 \times 10^6 \frac{\text{molec}}{\text{cm}^3 \text{s}}$		$5.9 \times 10^6 \frac{\text{molec}}{\text{cm}^3 \text{s}}$		$11.2 \times 10^6 \frac{\text{molec}}{\text{cm}^3 \text{s}}$		$5.0 \times 10^6 \frac{\text{molec}}{\text{cm}^3 \text{s}}$	
H ₂ O+O(¹ D)		36%		53%		61%		55%
NO+HO ₂		46%		13%		9%		9%
ISOOH+OH		10%		15%		0%		9%
H ₂ O ₂ +hv		4%		11%		19%		15%
HO ₂ +O ₃		2%		4%		6%		8%
ISOOH+hv		<1%		2%		0%		<1%
ISOP+O ₃		<1%		2%		0%		<1%
remaining		2%		2%		5%		4%
loss rate	$-8.2 \times 10^6 \frac{\text{molec}}{\text{cm}^3 \text{s}}$		$-5.9 \times 10^6 \frac{\text{molec}}{\text{cm}^3 \text{s}}$		$-11.2 \times 10^6 \frac{\text{molec}}{\text{cm}^3 \text{s}}$		$-5.0 \times 10^6 \frac{\text{molec}}{\text{cm}^3 \text{s}}$	
Isop+OH		39%		62%		0%		14%
CO+OH		13%		4%		35%		25%
ISOOH+OH		10%		15%		0%		9%
CH ₄ +OH		6%		2%		12%		9%
MVK+OH		4%		6%		1%		5%
MGLO+OH		3%		3%		1%		3%
HCHO+OH		3%		2%		7%		3%
MVKOOH+OH		<1%		<1%		5%		6%
CH ₃ OOH+OH		<1%		<1%		10%		6%
H ₂ O ₂ +OH		1%		<1%		10%		5%
remaining		19%		6%		19%		15%
OH observed	$(5.3 \pm 1.6) \times 10^6 \frac{\text{molec}}{\text{cm}^3}$		$(4.4 \pm 0.9) \times 10^6 \frac{\text{molec}}{\text{cm}^3}$		$(12.5 \pm 1.1) \times 10^6 \frac{\text{molec}}{\text{cm}^3}$		$(5.2 \pm 1.6) \times 10^6 \frac{\text{molec}}{\text{cm}^3}$	
OH modelled	$(2.1 \pm 0.8) \times 10^6 \frac{\text{molec}}{\text{cm}^3}$		$(0.4 \pm 0.1) \times 10^6 \frac{\text{molec}}{\text{cm}^3}$		$(10.1 \pm 0.7) \times 10^6 \frac{\text{molec}}{\text{cm}^3}$		$(3.2 \pm 2) \times 10^6 \frac{\text{molec}}{\text{cm}^3}$	

HO_x over the tropical rainforest: box model results

D. Kubistin et al.

Title Page

Abstract

Introduction

Conclusions

References

Tables

Figures



Back

Close

Full Screen / Esc

Printer-friendly Version

Interactive Discussion



Table 8. HO₂ budget based on a model analysis of measurement data.

	case 1: land morning BL 6 datapoints	case 2: land afternoon BL 23 datapoints	case 3: ocean noon (3.5±0.3) km 8 datapoints	case 4: land afternoon (3.3±0.4) km 20 datapoints
production rate	$6.4 \times 10^6 \frac{\text{molec}}{\text{cm}^3 \text{ s}}$	$4.3 \times 10^6 \frac{\text{molec}}{\text{cm}^3 \text{ s}}$	$9.2 \times 10^6 \frac{\text{molec}}{\text{cm}^3 \text{ s}}$	$3.4 \times 10^6 \frac{\text{molec}}{\text{cm}^3 \text{ s}}$
HCHO+hv	13%	36%	15%	18%
CO+OH	17%	6%	42%	35%
ISO ₂ +NO	32%	22%	0%	3%
ISO ₂ +ISO ₂	1%	8%	0%	<1%
CH ₃ O ₂ +NO	15%	5%	6%	8%
MVKO ₂ +NO	3%	3%	<1%	2%
HCHO+OH	4%	2%	8%	4%
ISOOH+hv	<1%	3%	0%	<1%
CH ₃ H ₆ O ₂ +NO	4%	<1%	0%	<1%
H ₂ O ₂ +OH	1%	<1%	12%	8%
remaining	14%	16%	16%	22%
loss rate	$-6.4 \times 10^6 \frac{\text{molec}}{\text{cm}^3 \text{ s}}$	$-4.3 \times 10^6 \frac{\text{molec}}{\text{cm}^3 \text{ s}}$	$-9.2 \times 10^6 \frac{\text{molec}}{\text{cm}^3 \text{ s}}$	$-3.4 \times 10^6 \frac{\text{molec}}{\text{cm}^3 \text{ s}}$
NO+HO ₂	59%	17%	12%	13%
HO ₂ +O ₃	3%	5%	7%	11%
ISO ₂ +HO ₂	15%	44%	0%	15%
HO ₂ +HO ₂	17%	21%	48%	30%
CH ₃ O ₂ +HO ₂	2%	3%	16%	13%
MVKO ₂ +HO ₂	2%	6%	6%	11%
HO ₂ +OH	1%	<1%	9%	4%
remaining	1%	1%	2%	3%
HO ₂ observed	$(6.3 \pm 0.5) \times 10^8 \frac{\text{molec}}{\text{cm}^3}$	$(10.2 \pm 1.9) \times 10^8 \frac{\text{molec}}{\text{cm}^3}$	$(5.7 \pm 0.6) \times 10^8 \frac{\text{molec}}{\text{cm}^3}$	$(4.7 \pm 1.5) \times 10^8 \frac{\text{molec}}{\text{cm}^3}$
HO ₂ modelled	$(2.9 \pm 0.2) \times 10^8 \frac{\text{molec}}{\text{cm}^3}$	$(2.6 \pm 0.6) \times 10^8 \frac{\text{molec}}{\text{cm}^3}$	$(7.0 \pm 1.2) \times 10^8 \frac{\text{molec}}{\text{cm}^3}$	$(3.3 \pm 1.3) \times 10^8 \frac{\text{molec}}{\text{cm}^3}$

HO_x over the tropical rainforest: box model results

D. Kubistin et al.

Title Page

Abstract Introduction

Conclusions References

Tables Figures

◀ ▶

◀ ▶

Back Close

Full Screen / Esc

Printer-friendly Version

Interactive Discussion



HO_x over the tropical rainforest: box model results

D. Kubistin et al.

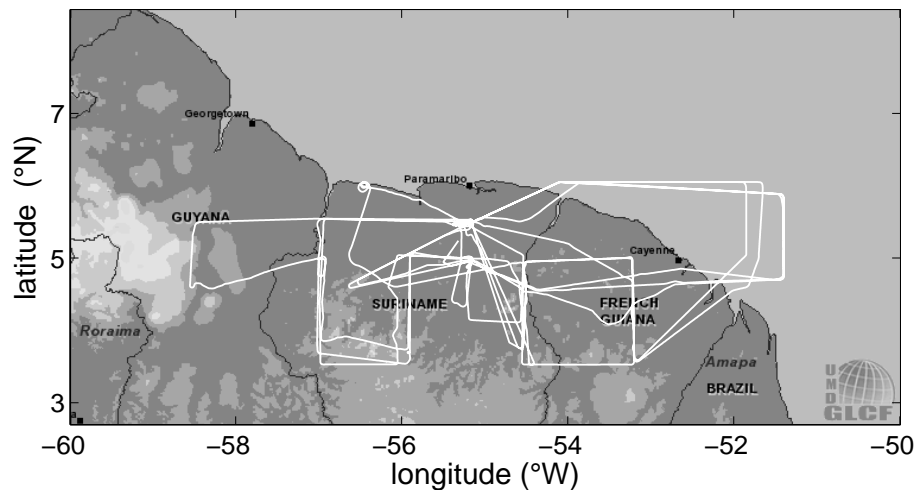


Fig. 1. Flighttracks over the Guyanas during the GABRIEL campaign (map taken from Earth Science Data Interface (ESDI), University of Maryland).

[Title Page](#)[Abstract](#)[Introduction](#)[Conclusions](#)[References](#)[Tables](#)[Figures](#)[◀](#)[▶](#)[◀](#)[▶](#)[Back](#)[Close](#)[Full Screen / Esc](#)[Printer-friendly Version](#)[Interactive Discussion](#)

HO_x over the tropical rainforest: box model results

D. Kubistin et al.

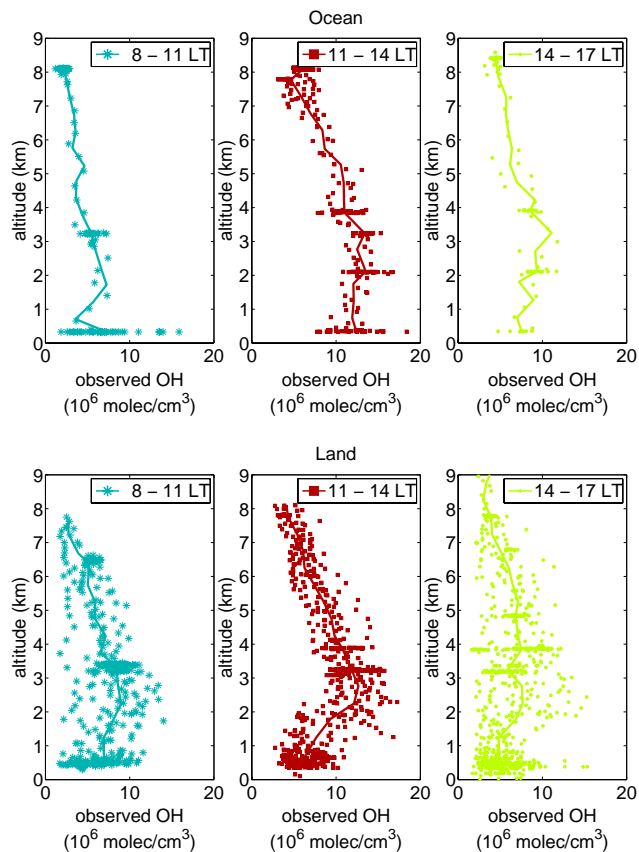


Fig. 2. OH (30 s average) observed for all flights as a function of altitude. The thick line denotes the mean values in 500 m bins. Upper row represents the situation over the ocean for different times of the day (left to right panel), lower row shows the situation over land.

[Title Page](#)[Abstract](#)[Introduction](#)[Conclusions](#)[References](#)[Tables](#)[Figures](#)[◀](#)[▶](#)[◀](#)[▶](#)[Back](#)[Close](#)[Full Screen / Esc](#)[Printer-friendly Version](#)[Interactive Discussion](#)

HO_x over the tropical rainforest: box model results

D. Kubistin et al.

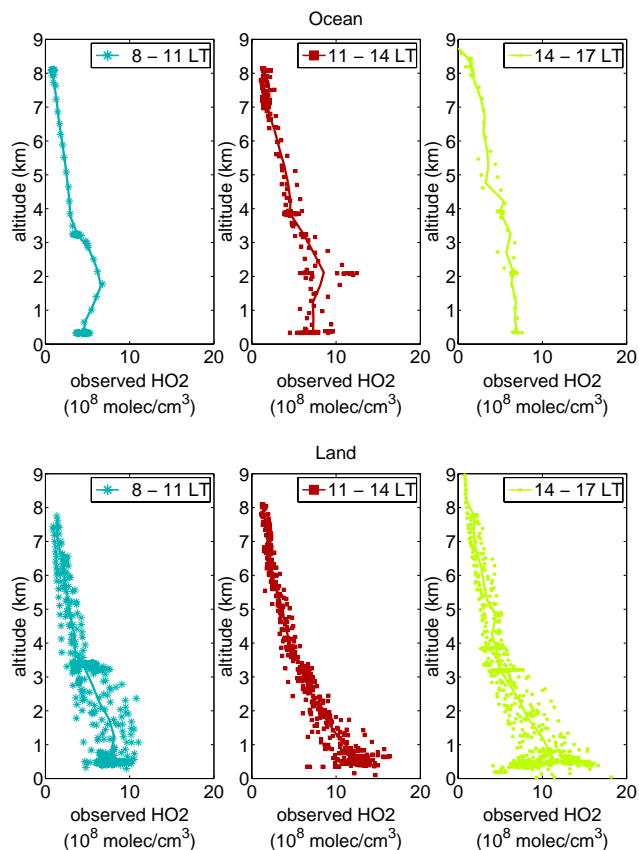


Fig. 3. HO₂ (30 s average) observed for all flights as a function of altitude. The thick line denotes the mean values in 500 m bins. Upper row represents the situation over the ocean for different times of the day (left to right panel), lower row shows the situation over land.

[Title Page](#)[Abstract](#)[Introduction](#)[Conclusions](#)[References](#)[Tables](#)[Figures](#)[◀](#)[▶](#)[◀](#)[▶](#)[Back](#)[Close](#)[Full Screen / Esc](#)[Printer-friendly Version](#)[Interactive Discussion](#)

HO_x over the tropical rainforest: box model results

D. Kubistin et al.

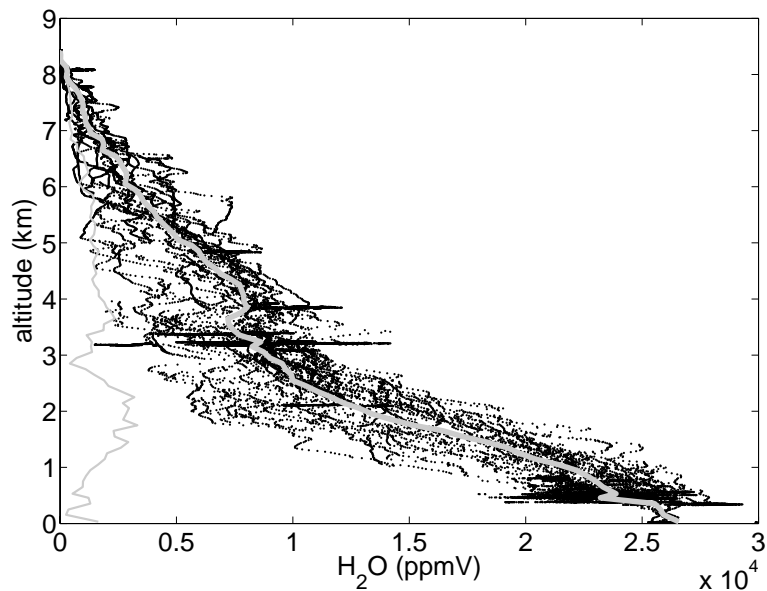


Fig. 4. Observed H₂O (1 s resolution) data for all flights as a function of altitude. The thick grey line denotes the mean values for 100 m bins, the thin grey line the standard deviation.

[Title Page](#)[Abstract](#)[Introduction](#)[Conclusions](#)[References](#)[Tables](#)[Figures](#)[◀](#)[▶](#)[◀](#)[▶](#)[Back](#)[Close](#)[Full Screen / Esc](#)[Printer-friendly Version](#)[Interactive Discussion](#)

HO_x over the tropical rainforest: box model results

D. Kubistin et al.

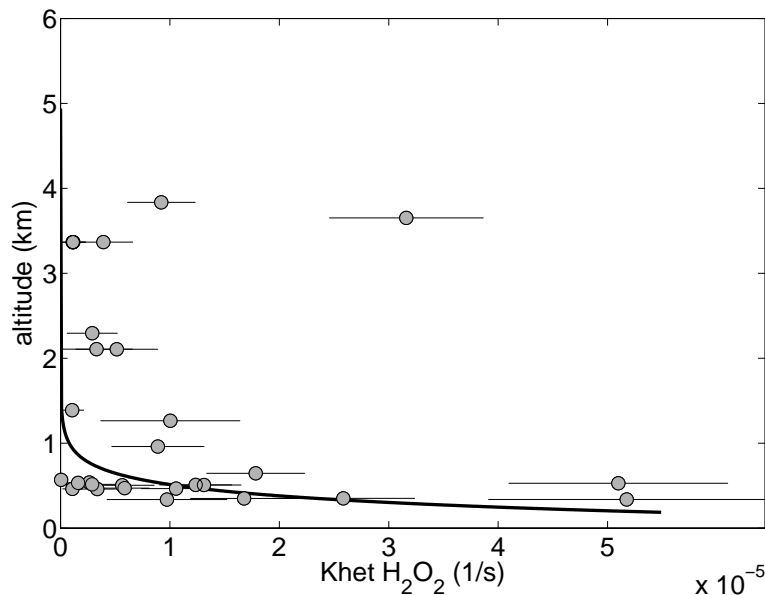


Fig. 5. Calculated heterogeneous removal rate $k_{\text{het}}(\text{H}_2\text{O}_2)$ as a function of altitude, as caused by wet and dry deposition processes.

[Title Page](#)[Abstract](#)[Introduction](#)[Conclusions](#)[References](#)[Tables](#)[Figures](#)[◀](#)[▶](#)[◀](#)[▶](#)[Back](#)[Close](#)[Full Screen / Esc](#)[Printer-friendly Version](#)[Interactive Discussion](#)

HO_x over the tropical rainforest: box model results

D. Kubistin et al.

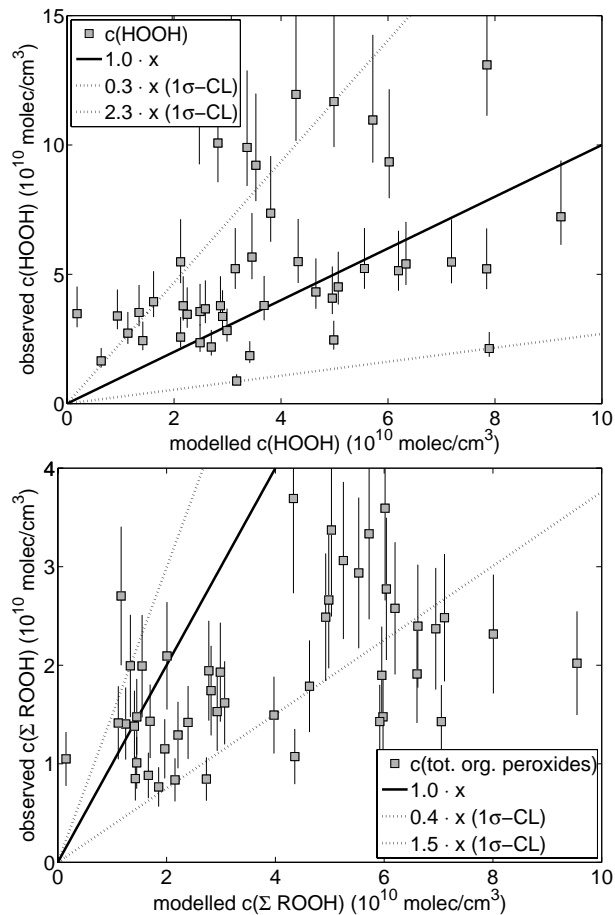


Fig. 6. Observed and modelled data for hydrogen peroxide ($\text{H}_2\text{O}_2=\text{HOOH}$) and total organic peroxides (ΣROOH). The solid line represent perfect agreement, the dashed lines bound the 1σ confidence level ($1\sigma\text{-CL}$).

[Title Page](#)[Abstract](#)[Introduction](#)[Conclusions](#)[References](#)[Tables](#)[Figures](#)[◀](#)[▶](#)[◀](#)[▶](#)[Back](#)[Close](#)[Full Screen / Esc](#)[Printer-friendly Version](#)[Interactive Discussion](#)

HO_x over the tropical rainforest: box model results

D. Kubistin et al.

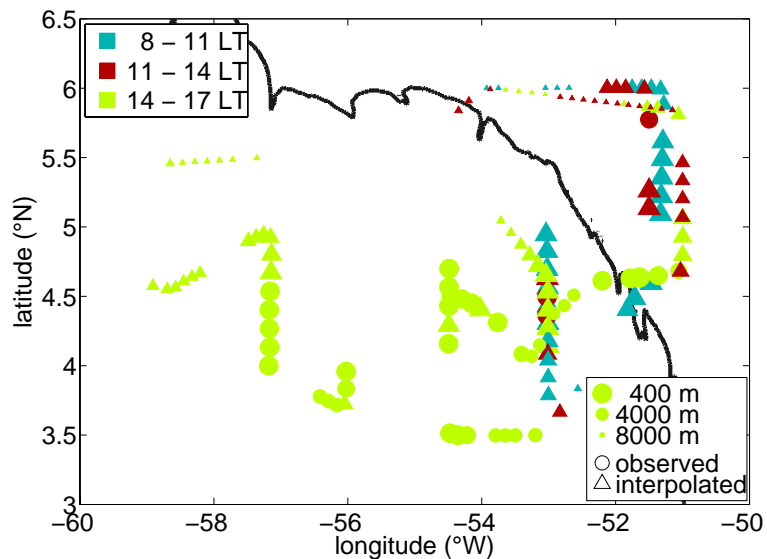


Fig. 7. Measurement locations of datapoints used to model OH and HO₂. The black line represents the coastline.

[Title Page](#)[Abstract](#)[Introduction](#)[Conclusions](#)[References](#)[Tables](#)[Figures](#)[◀](#)[▶](#)[◀](#)[▶](#)[Back](#)[Close](#)[Full Screen / Esc](#)[Printer-friendly Version](#)[Interactive Discussion](#)

HO_x over the tropical rainforest: box model results

D. Kubistin et al.

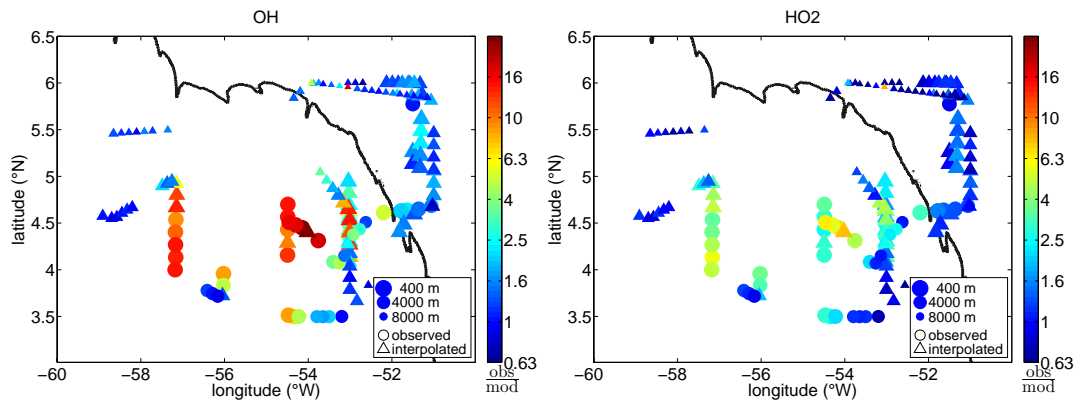


Fig. 8. Ratio of observed to simulated OH and HO₂. The black line represents the coastline.

[Title Page](#)[Abstract](#)[Introduction](#)[Conclusions](#)[References](#)[Tables](#)[Figures](#)[◀](#)[▶](#)[◀](#)[▶](#)[Back](#)[Close](#)[Full Screen / Esc](#)[Printer-friendly Version](#)[Interactive Discussion](#)

HO_x over the tropical rainforest: box model results

D. Kubistin et al.

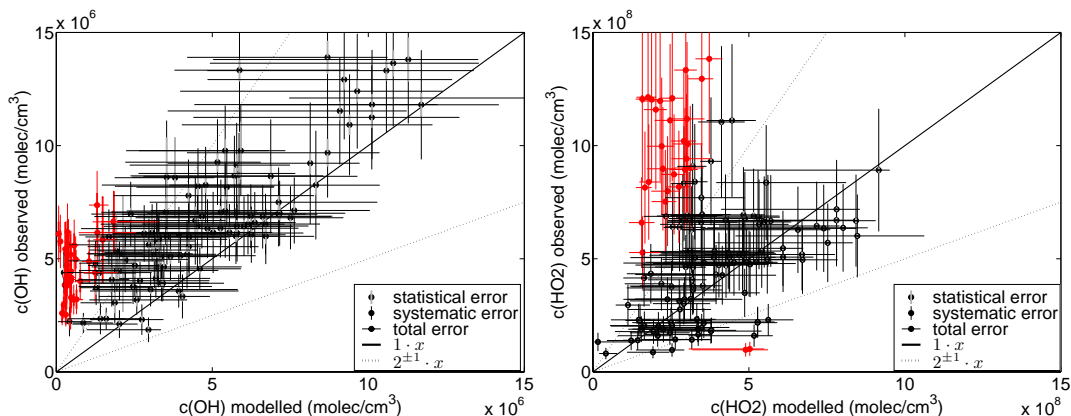


Fig. 9. Error estimates for the simulations due to measurement uncertainties. The solid line represents the perfect match of simulation and observations. The dashed lines correspond to ratios of 1:2 and 2:1. Red points illustrate deviations by more than a factor of $2^{\pm 1}$.

[Title Page](#)[Abstract](#)[Introduction](#)[Conclusions](#)[References](#)[Tables](#)[Figures](#)[◀](#)[▶](#)[◀](#)[▶](#)[Back](#)[Close](#)[Full Screen / Esc](#)[Printer-friendly Version](#)[Interactive Discussion](#)

HO_x over the tropical rainforest: box model results

D. Kubistin et al.

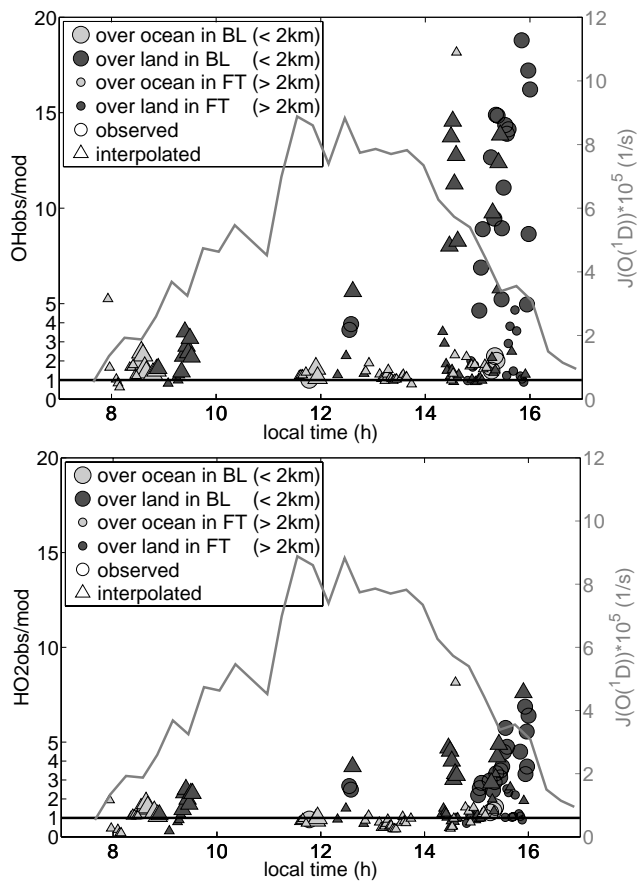


Fig. 10. Comparison of measurements and model results as a function of time, divided into two altitude regions: boundary layer (BL) < 2 km and free troposphere (FT) > 2 km.

[Title Page](#)[Abstract](#)[Introduction](#)[Conclusions](#)[References](#)[Tables](#)[Figures](#)[◀](#)[▶](#)[◀](#)[▶](#)[Back](#)[Close](#)[Full Screen / Esc](#)[Printer-friendly Version](#)[Interactive Discussion](#)

HO_x over the tropical rainforest: box model results

D. Kubistin et al.

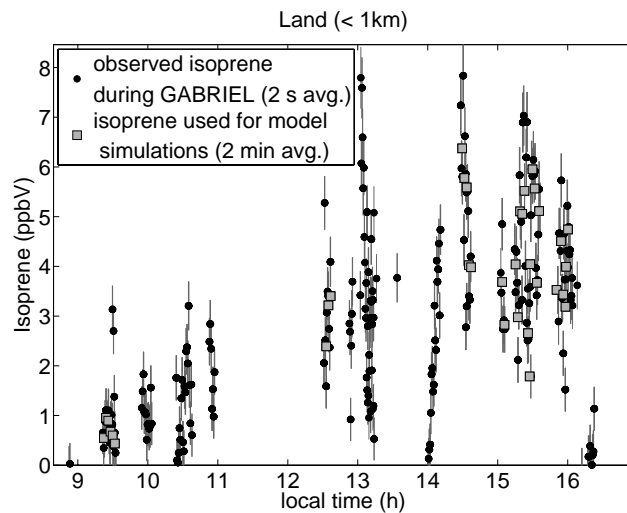


Fig. 11. Observed isoprene mixing ratios with their measurement uncertainties for altitudes <1 km over the rainforest.

[Title Page](#)[Abstract](#)[Introduction](#)[Conclusions](#)[References](#)[Tables](#)[Figures](#)[◀](#)[▶](#)[◀](#)[▶](#)[Back](#)[Close](#)[Full Screen / Esc](#)[Printer-friendly Version](#)[Interactive Discussion](#)

HO_x over the tropical rainforest: box model results

D. Kubistin et al.

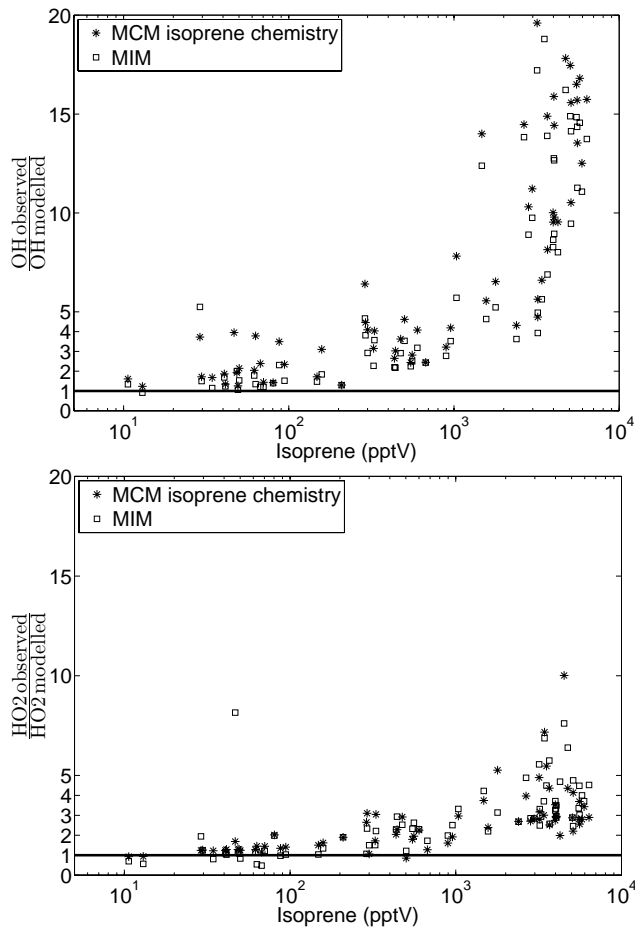


Fig. 12. Deviations between observations and model results as a function of isoprene mixing ratios.

[Title Page](#)[Abstract](#)[Introduction](#)[Conclusions](#)[References](#)[Tables](#)[Figures](#)[◀](#)[▶](#)[◀](#)[▶](#)[Back](#)[Close](#)[Full Screen / Esc](#)[Printer-friendly Version](#)[Interactive Discussion](#)

HO_x over the tropical rainforest: box model results

D. Kubistin et al.

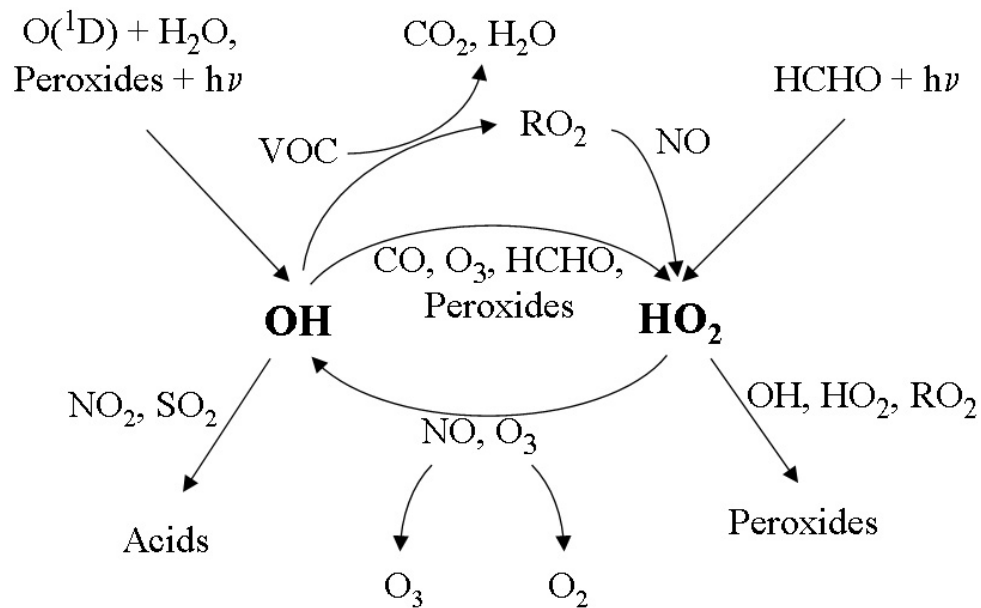


Fig. 13. Schematic representation of HO_x cycling.

Title Page

Abstract

Introduction

Conclusions

References

Tables

Figures

◀

▶

◀

▶

Back

Close

Full Screen / Esc

Printer-friendly Version

Interactive Discussion



HO_x over the tropical rainforest: box model results

D. Kubistin et al.

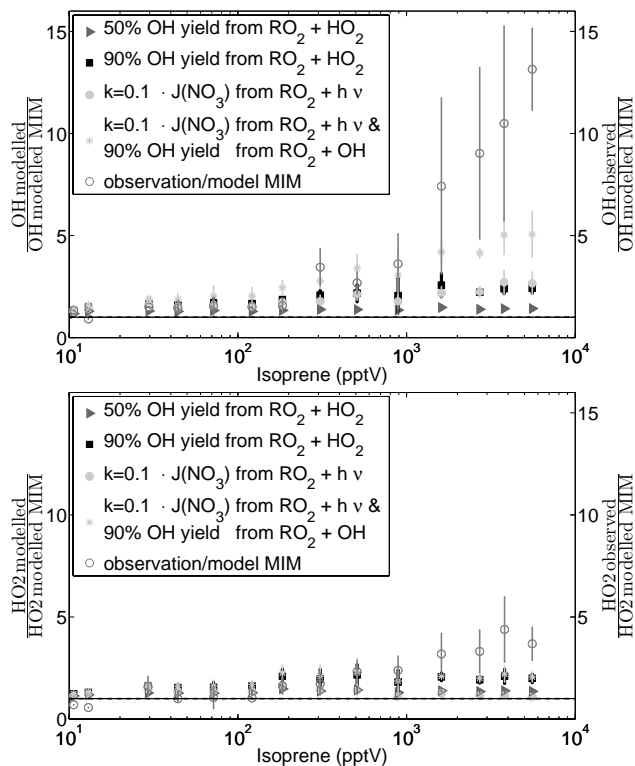


Fig. 14. Comparison of observed and modelled HO_x based on selected changes in the MECCA chemistry scheme. Values are binned in isoprene mixing ratios (x) of $\Delta \ln x = 0.5$.

Title Page

Abstract

Introduction

Conclusions

References

Tables

Figures

◀

▶

◀

▶

Back

Close

Full Screen / Esc

Printer-friendly Version

Interactive Discussion



HO_x over the tropical rainforest: box model results

D. Kubistin et al.

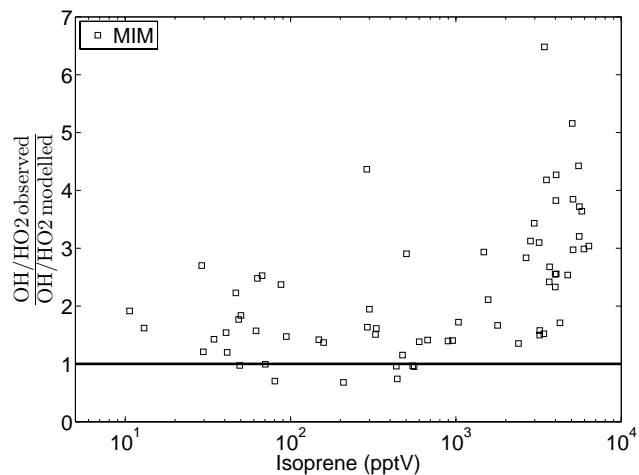


Fig. 15. Deviation of the ratio OH/HO₂ between observation and model as a function of isoprene.

[Title Page](#)[Abstract](#)[Introduction](#)[Conclusions](#)[References](#)[Tables](#)[Figures](#)[◀](#)[▶](#)[◀](#)[▶](#)[Back](#)[Close](#)[Full Screen / Esc](#)[Printer-friendly Version](#)[Interactive Discussion](#)

HO_x over the tropical rainforest: box model results

D. Kubistin et al.

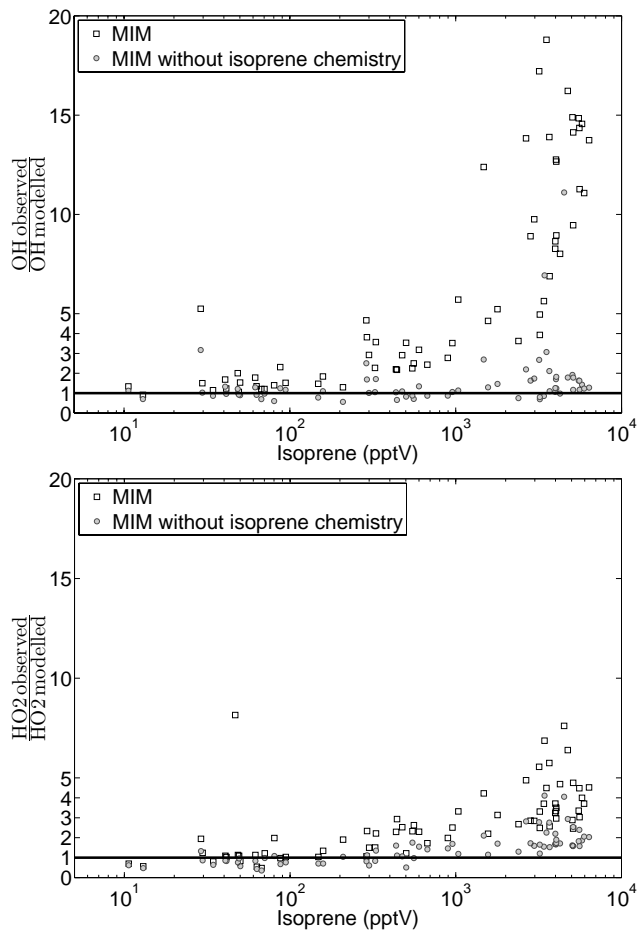


Fig. 16. Ratio of observed and modelled OH and HO₂ concentrations as a function of isoprene and other conditions observed simultaneously with isoprene.

[Title Page](#)[Abstract](#)[Introduction](#)[Conclusions](#)[References](#)[Tables](#)[Figures](#)[◀](#)[▶](#)[◀](#)[▶](#)[Back](#)[Close](#)[Full Screen / Esc](#)[Printer-friendly Version](#)[Interactive Discussion](#)

HO_x over the tropical rainforest: box model results

D. Kubistin et al.

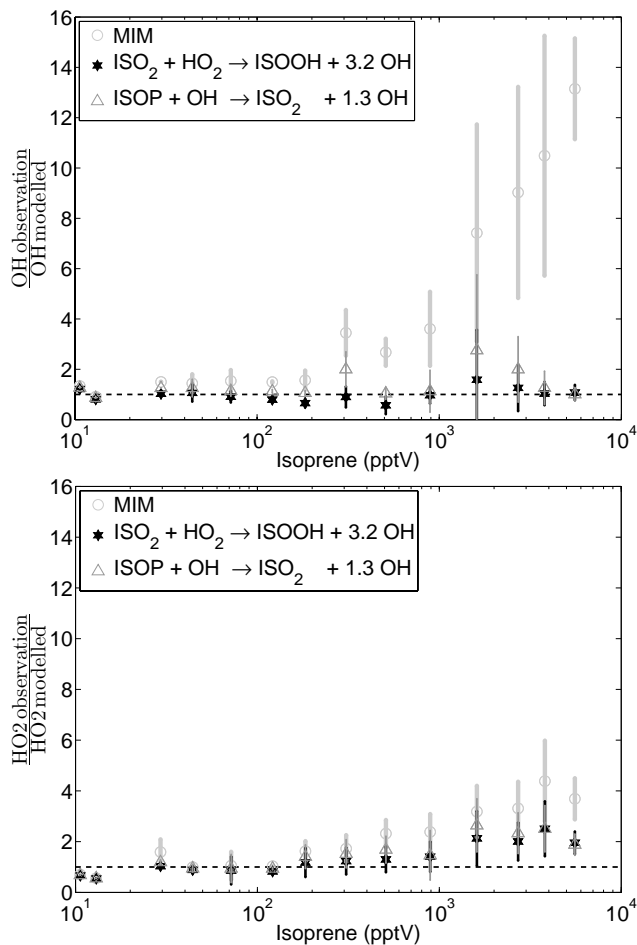


Fig. 17. Comparison between observation and a model run including the additional HO_x reaction: $\text{ISOOH} + \text{HO}_2 \rightarrow \text{ISOOH} + n\text{OH}$ and $\text{ISOP} + \text{OH} \rightarrow \text{ISO}_2 + m\text{OH}$. Values are binned in isoprene mixing ratios (x) of $\Delta \ln x = 0.5$.

[Title Page](#)
[Abstract](#)
[Introduction](#)
[Conclusions](#)
[References](#)
[Tables](#)
[Figures](#)
[◀](#)
[▶](#)
[◀](#)
[▶](#)
[Back](#)
[Close](#)
[Full Screen / Esc](#)
[Printer-friendly Version](#)
[Interactive Discussion](#)
